AIMS Mathematics, 11(11): 38044–38082.
DOI: 10.3934/math.20261470
Received: 13 August 2026
Revised: 10 October 2026
Accepted: 23 October 2026
Published: 16 November 2026

http://www.aimspress.com/journal/Math

Research article

Exponential exponentiated modeling of unobserved heterogeneity: An alternative to gamma frailty

Guillermo Martinez-Florez[1], **Javier Ramirez-Montoya**[1,*] **and Rodrigo M. R. de Medeiros**[2]

[1] Department of Mathematics and Statistics, University of Córdoba, Montería, Córdoba, 230002, Colombia

[2] Department of Statistics, Federal University of Rio Grande do Norte, Lagoa Nova, 59078-970, Natal, RN, Brazil

* **Correspondence:** Email: jaramirez@correo.unicordoba.edu.co.

Abstract: Frailty models are widely used in survival analysis to account for unobserved heterogeneity among individuals. Although the gamma distribution is the most commonly adopted frailty model because of its analytical tractability, alternative distributions may provide greater modeling flexibility while preserving convenient inferential properties. In this paper, we introduce a frailty model based on the exponentiated exponential distribution as an alternative to the classical gamma frailty. The proposed frailty is reparameterized to have unit mean, ensuring model identifiability and a common population interpretation. Closed-form expressions are derived for the frailty variance, Laplace transform, and population-level survival, density, cumulative distribution, and hazard functions. A unified likelihood-based inference framework is developed, including maximum likelihood estimation, asymptotic inference, confidence intervals, likelihood ratio tests for the presence of frailty, and empirical Bayes prediction of individual frailty effects. The methodology is presented for general survival-model specifications and illustrated for Weibull and log-normal survival models. The finite-sample performance of the proposed estimators is evaluated through an extensive Monte Carlo simulation study under different sample sizes, censoring proportions, survival-model specifications, and heterogeneity levels. The simulation results show generally satisfactory estimation of the regression effects under low and moderate censoring, while also highlighting the greater sensitivity of frailty-variance estimation and individual frailty prediction to severe censoring and distributional misspecification. Overall, the proposed model provides a flexible and analytically tractable alternative to the classical gamma frailty model, without implying systematic superiority of either frailty specification.

Keywords: survival analysis; frailty models; exponentiated exponential distribution; unobserved heterogeneity; maximum likelihood estimation; Weibull model; log-normal model
Mathematics Subject Classification: 62N01, 62N02, 62F10, 60E05

Abbreviations

The following abbreviations are used in this manuscript:

Abbreviation	Meaning
EE	Exponentiated exponential
PH	Proportional hazards
AFT	Accelerated failure time
EB	Empirical Bayes
RMSE	Root mean squared error
SD	Standard deviation
AIC	Akaike information criterion
AICc	Corrected Akaike information criterion
HQIC	Hannan-Quinn information criterion
SIVIGILA	Colombian National Public Health Surveillance System

1. Introduction

Frailty models have become one of the principal approaches for incorporating unobserved heterogeneity into survival analysis. In these models, differences between individuals that cannot be explained by the observed covariates are represented through a positive latent random variable. Depending on the formulation, frailty may represent subject-specific residual heterogeneity or may be shared among individuals belonging to the same cluster, in which case it also induces dependence among survival times [1–3].

The choice of the frailty distribution plays a fundamental role in determining both the interpretation and the analytical tractability of the resulting survival model. Among the available alternatives, the gamma frailty model has become the most widely used owing to its closed-form Laplace transform, which leads to explicit expressions for marginal survival quantities and greatly simplifies likelihood-based inference. Other distributions, including the log-normal, inverse Gaussian, and positive stable families, have also been proposed to accommodate different patterns of unobserved heterogeneity [3–5]. Nevertheless, several alternative frailty specifications require numerical approximations for marginal quantities or lead to more complex likelihood calculations.

Frailty modeling has evolved considerably from classical individual-level and shared-frailty formulations to correlated, multivariate, and more flexible distributional constructions [3, 6, 7]. More recently, considerable attention has been devoted to frailty distributions capable of representing more complex forms of heterogeneity while retaining tractable likelihood-based inference [8–10]. For example, [9] introduced a double exponential gamma frailty model for clustered survival data, whereas [10] proposed a logarithmic gamma frailty model for first-failure times with heavy-tailed heterogeneity. Recent contributions have also extended shared-frailty regression models for explicitly clustered survival outcomes. Kiprotich et al. [11] proposed a shared frailty model based on a finite mixture of inverse Gaussian distributions for multivariate lifetimes. The hierarchical mixture representation facilitates estimation through an expectation-maximization algorithm, while its closed-form Laplace transform permits an explicit characterization of within-cluster dependence.

More recently, Kiprotich et al. [12] introduced a broader frailty regression construction based on mixtures of Birnbaum-Saunders distributions, considering both parametric and semiparametric formulations for clustered survival data. These developments illustrate the growing interest in flexible frailty distributions that combine richer latent heterogeneity structures with computationally tractable inference.

The present proposal is related to this literature through its emphasis on flexible distributional modeling of latent heterogeneity, but its objective and data structure are different. The models of [11, 12] are shared-frailty constructions in which a common latent effect induces dependence among survival times within a cluster. In contrast, the framework considered here assigns an independent frailty V_i to each individual. Consequently, the proposed EE frailty does not induce between-subject dependence and is intended to represent residual individual-level heterogeneity remaining after adjustment for observed covariates. Population-level heterogeneity is identified through the marginal likelihood under the assumed survival and frailty distributions, whereas individual frailty values are treated as latent quantities and may subsequently be summarized through model-based empirical Bayes predictions.

Recent developments outside the frailty literature also illustrate the broader interest in flexible parametric approaches for survival and lifetime data. Ishag et al. [13] proposed a fully parametric Yang-Prentice regression model capable of accommodating crossing survival curves, whereas Elsherpieny and Abdel-Hakim [14] considered inference for the alpha-power exponential distribution under unified hybrid censoring. These contributions further illustrate the continuing development of tractable parametric models for survival and censored lifetime data.

The exponentiated exponential (EE) distribution, originally investigated by [15], constitutes a flexible lifetime distribution with simple analytical expressions for its probability density, cumulative distribution, survival, and hazard functions. Its shape parameter allows different distributional forms while retaining considerable mathematical simplicity. Despite these appealing properties, the EE distribution has received little attention as a frailty distribution.

The novelty of the present proposal lies in adapting the exponentiated exponential family to the frailty setting through a unit-mean reparameterization that preserves a single parameter governing the magnitude of residual heterogeneity. In contrast to several flexible frailty distributions whose marginal likelihoods require numerical integration, the standardized EE frailty retains a closed-form Laplace transform under the multiplicative-hazard formulation, yielding explicit marginal survival, density, and hazard functions. At the same time, the proposal differs from recent shared-frailty constructions for clustered survival data because it is formulated here as an individual-specific frailty distribution for residual subject-level heterogeneity. The aim is therefore not to replace the gamma frailty universally, but to provide a distinct, analytically tractable parametric alternative with a different latent distributional shape.

Motivated by these considerations, we introduce the standardized EE distribution as an alternative frailty law. The reparameterization is constructed so that the frailty variable has unit mean, thereby satisfying the usual scale-identifiability constraint while preserving a single parameter controlling the degree of residual heterogeneity. Under the proportional hazards formulation, the resulting model admits a closed-form Laplace transform and consequently explicit marginal survival, density, distribution, and hazard functions. The same frailty distribution is also considered within the log-normal accelerated failure time formulation through numerical marginalization of the individual

likelihood contributions.

The main contributions of this paper are summarized as follows. First, we introduce the standardized EE distribution as a frailty distribution and derive its principal probabilistic properties. Second, under the proportional hazards formulation, explicit expressions are obtained for the Laplace transform and the corresponding marginal survival, density, distribution, and hazard functions. Third, likelihood-based estimation, testing for residual heterogeneity, and empirical Bayes prediction of individual frailty effects are developed. Fourth, the finite-sample behavior of the proposed specification is investigated through an extensive Monte Carlo simulation study and compared with the classical gamma frailty model. Finally, the methodology is illustrated using survival data from pulmonary tuberculosis surveillance.

The remainder of this paper is organized as follows: Section 2 introduces the proposed EE frailty model and develops its main probabilistic properties. Section 3 presents likelihood-based inference procedures and discusses hypothesis testing for residual heterogeneity. Section 4 presents the simulation study, and Section 5 illustrates the methodology using a real-data application. Finally, concluding remarks are given in Section 6. Technical derivations and additional simulation results are provided in the Appendix.

2. Proposed model

This section introduces the proposed EE frailty distribution and develops its main probabilistic properties. We first consider a multiplicative-hazard frailty formulation and derive the corresponding closed-form marginal quantities through the Laplace transform of the EE distribution. The proportional hazards model is then obtained as an important special case. We subsequently distinguish this construction from the log-normal accelerated failure time formulation used in the simulation study and empirical application. Finally, we derive the conditional frailty distributions and empirical Bayes predictors under the two formulations.

A positive continuous random variable V is said to follow an EE distribution with shape parameter $\alpha > 0$ and scale parameter $\lambda > 0$ if its probability density function is given by

$$f(v;\alpha,\lambda) = \alpha\lambda(1-\mathrm{e}^{-\lambda v})^{\alpha-1}\mathrm{e}^{-\lambda v}, \quad v > 0.$$

As discussed in the previous section, the EE distribution is reparameterized to satisfy the identifiability condition $\mathrm{E}(V) = 1$. Under this parameterization, the frailty variable depends on a single shape parameter α, while the scale parameter becomes $\lambda = \lambda(\alpha) = \psi(\alpha+1) - \psi(1)$, where $\psi(\cdot)$ is the digamma function. Consequently, the frailty density is given by

$$f_{EE}(v;\alpha) = \alpha\left[\psi(\alpha+1)-\psi(1)\right] e^{-\left[\psi(\alpha+1)-\psi(1)\right]v}\left(1-e^{-\left[\psi(\alpha+1)-\psi(1)\right]v}\right)^{\alpha-1}, \quad v > 0.$$

We write $V \sim \mathrm{EE}(\alpha, \lambda(\alpha))$. The corresponding variance of $V \sim \mathrm{EE}(\alpha, \lambda(\alpha))$ can be expressed as

$$\mathrm{Var}(V) = \sigma_V^2 = \frac{\psi'(1)-\psi'(\alpha+1)}{\left[\psi(1)-\psi(\alpha+1)\right]^2},$$

where $\psi'(\cdot)$ denotes the trigamma function. The parameter α controls the magnitude of frailty heterogeneity through this variance. In particular, larger values of α imply smaller values of

Var(V), so that the frailty distribution becomes increasingly concentrated around its unit mean. Conversely, smaller values of α correspond to greater frailty dispersion and therefore stronger residual heterogeneity. In the limit $\alpha \to \infty$, Var(V) $\to 0$ and the frailty distribution degenerates at $V = 1$, recovering the corresponding model without frailty. Thus, although estimation is parameterized in terms of α, Var(V) provides the more direct measure of the magnitude of residual heterogeneity.

2.1. Covariates and frailty structure

Let $\mathbf{X} = (X_1, \ldots, X_p)^\top$ denote a vector of observed covariates. Two related but distinct regression formulations are considered in this article. The first is the multiplicative-hazard frailty formulation, which includes the proportional hazards model as a special case and leads to the closed-form Laplace-transform results developed below. The second is a log-normal accelerated failure time (AFT) formulation, used in the simulation study and empirical application, in which the frailty acts on the time scale rather than multiplicatively on the hazard.

2.1.1. Multiplicative-hazard formulation

Let $h_*(t \mid \mathbf{X})$ denote a covariate-adjusted hazard function before the introduction of frailty. Conditional on the positive latent frailty $V = v$, define

$$h(t \mid \mathbf{X}, V = v) = v\, h_*(t \mid \mathbf{X}), \qquad t > 0. \tag{2.1}$$

If $H_*(t \mid \mathbf{X}) = \int_0^t h_*(s \mid \mathbf{X})\, ds$, then the corresponding conditional survival function is

$$S(t \mid \mathbf{X}, V = v) = \exp\{-vH_*(t \mid \mathbf{X})\}. \tag{2.2}$$

The proportional hazards specification is obtained by setting

$$h_*(t \mid \mathbf{X}) = h_0(t) \exp(\mathbf{X}^\top \boldsymbol{\beta}), \qquad H_*(t \mid \mathbf{X}) = H_0(t) \exp(\mathbf{X}^\top \boldsymbol{\beta}). \tag{2.3}$$

Thus, under proportional hazards,

$$h(t \mid \mathbf{X}, V = v) = vh_0(t) \exp(\mathbf{X}^\top \boldsymbol{\beta}).$$

Since V is unobserved, the marginal survival function under the multiplicative-hazard formulation is obtained by integrating over the frailty distribution:

$$S_m(t \mid \mathbf{X}) = \mathbb{E}[\exp\{-VH_*(t \mid \mathbf{X})\}] = L_V\{H_*(t \mid \mathbf{X})\}, \tag{2.4}$$

where $L_V(\cdot)$ denotes the Laplace transform of V. For the standardized EE frailty distribution, let $\lambda(\alpha) = \psi(\alpha + 1) - \psi(1)$. Its Laplace transform is

$$L_V(s) = \int_0^\infty e^{-sv} \alpha\lambda(\alpha) \left(1 - e^{-\lambda(\alpha)v}\right)^{\alpha-1} e^{-\lambda(\alpha)v}\, dv. \tag{2.5}$$

Using the transformation $z = e^{-\lambda(\alpha)v}$, the preceding expression becomes

$$L_V(s) = \alpha \int_0^1 (1 - z)^{\alpha-1} z^{s/\lambda(\alpha)}\, dz = \alpha B\left(\alpha, 1 + \frac{s}{\lambda(\alpha)}\right), \tag{2.6}$$

where $B(\cdot,\cdot)$ denotes the beta function. Consequently, under the multiplicative-hazard formulation,

$$S_m(t \mid \mathbf{X}) = \alpha B\left(\alpha, 1 + \frac{H_*(t \mid \mathbf{X})}{\lambda(\alpha)}\right). \tag{2.7}$$

Under the proportional hazards specification in (2.3), this reduces to

$$S_m(t \mid \mathbf{X}) = \alpha B\left(\alpha, 1 + \frac{H_0(t)\exp(\mathbf{X}^\top \boldsymbol{\beta})}{\lambda(\alpha)}\right). \tag{2.8}$$

Thus, the standardized EE frailty distribution provides a closed-form marginal survival function under the multiplicative-hazard construction, which is one of the principal analytical advantages of the proposed specification. Consequently, the closed-form marginal expressions derived in the following subsections apply to the multiplicative-hazard construction. The analytical score and observed-information expressions presented in Appendix B are further specialized to the proportional hazards representation in (2.3).

2.1.2. Log-normal AFT formulation

The log-normal model considered later in the simulation study and empirical application is formulated on the accelerated failure time scale. Specifically,

$$\log(T_i \mid V_i = v, \mathbf{X}_i) = \mu + \mathbf{X}_i^\top \boldsymbol{\beta} - \log(v) + \sigma Z_i, \qquad Z_i \sim N(0,1), \tag{2.9}$$

where $\sigma > 0$. Define

$$z_i(v) = \frac{\log(t_i) - \mu - \mathbf{X}_i^\top \boldsymbol{\beta} + \log(v)}{\sigma}. \tag{2.10}$$

Conditional on $V_i = v$, the density and survival functions are

$$f(t_i \mid v, \mathbf{X}_i) = \frac{\phi\{z_i(v)\}}{\sigma t_i}, \qquad S(t_i \mid v, \mathbf{X}_i) = 1 - \Phi\{z_i(v)\}, \tag{2.11}$$

where $\phi(\cdot)$ and $\Phi(\cdot)$ denote the standard normal density and distribution functions, respectively. In this formulation, V rescales survival time and does not act as a simple multiplicative factor on the hazard. Equivalently, conditional on the covariates, a unit increase in $\log(V)$ shifts $\log(T)$ downward by one unit, so that larger frailty values correspond to shorter survival times on the AFT scale. Therefore, the Laplace-transform expressions derived for (2.1) do not apply directly. Instead, marginal quantities are obtained by integrating the conditional AFT density or survival function over the frailty distribution:

$$f_m(t_i \mid \mathbf{X}_i) = \int_0^\infty f(t_i \mid v, \mathbf{X}_i) g(v)\, dv, \; S_m(t_i \mid \mathbf{X}_i) = \int_0^\infty S(t_i \mid v, \mathbf{X}_i) g(v)\, dv. \tag{2.12}$$

These integrals are evaluated numerically in the simulation study and real-data application. Thus, the log-normal specification belongs to the same broader frailty framework in the sense that a positive latent variable represents residual subject-level heterogeneity, but its regression interpretation is AFT rather than proportional hazards. Consequently, the Laplace-transform simplifications available under the multiplicative-hazard formulation do not apply, and the marginal quantities are evaluated numerically.

2.2. Marginal quantities under the multiplicative-hazard formulation

We now return to the multiplicative-hazard formulation. For notational convenience, define

$$q(t, \mathbf{X}) = 1 + \frac{H_*(t \mid \mathbf{X})}{\lambda(\alpha)}, \qquad \lambda(\alpha) = \psi(\alpha + 1) - \psi(1). \tag{2.13}$$

Then $S_m(t \mid \mathbf{X}) = \alpha B\{\alpha, q(t, \mathbf{X})\}$. Differentiating the marginal survival function with respect to time gives

$$f_m(t \mid \mathbf{X}) = \frac{\alpha h_*(t \mid \mathbf{X})}{\lambda(\alpha)} B\{\alpha, q(t, \mathbf{X})\} \left[\psi\{\alpha + q(t, \mathbf{X})\} - \psi\{q(t, \mathbf{X})\}\right], \qquad t > 0. \tag{2.14}$$

The marginal distribution function is therefore $F_m(t \mid \mathbf{X}) = 1 - \alpha B\{\alpha, q(t, \mathbf{X})\}$, and the corresponding marginal hazard function is

$$h_m(t \mid \mathbf{X}) = \frac{h_*(t \mid \mathbf{X})}{\lambda(\alpha)} \left[\psi\{\alpha + q(t, \mathbf{X})\} - \psi\{q(t, \mathbf{X})\}\right], \qquad t > 0. \tag{2.15}$$

Under proportional hazards, $h_*(t \mid \mathbf{X}) = h_0(t) \exp(\mathbf{X}^\top \boldsymbol{\beta})$ and $H_*(t \mid \mathbf{X}) = H_0(t) \exp(\mathbf{X}^\top \boldsymbol{\beta})$, so that the preceding expressions immediately provide the corresponding PH marginal survival, density, distribution, and hazard functions. The conditional frailty distributions depend on whether an individual is right-censored or experiences the event. Under proportional hazards, closed-form expressions can be obtained from derivatives of the Laplace transform. Under the log-normal AFT formulation, by contrast, the posterior frailty distribution is obtained from the complete individual likelihood contribution and evaluated numerically. These two cases are developed in the following subsection.

2.3. Prediction of individual frailties

Under the proportional hazards formulation, define $h(t \mid \mathbf{X}) = h_0(t) \exp(\mathbf{X}^\top \boldsymbol{\beta})$ and $H(t \mid \mathbf{X}) = H_0(t) \exp(\mathbf{X}^\top \boldsymbol{\beta})$. Conditional on $V = v$, the corresponding hazard and cumulative hazard are $vh(t \mid \mathbf{X})$ and $vH(t \mid \mathbf{X})$, respectively. For notational convenience, under this PH specification define

$$q(t, \mathbf{X}) = 1 + \frac{H_0(t) \exp(\mathbf{X}^\top \boldsymbol{\beta})}{\lambda(\alpha)}. \tag{2.16}$$

As shown previously, the Laplace transform of the EE frailty distribution evaluated at the cumulative hazard is $L_V\{H(t \mid \mathbf{X})\} = \alpha B(\alpha, q(t, \mathbf{X}))$. For an individual who is right-censored at time t, the observed information is $T > t$. The corresponding posterior frailty density is

$$g(v \mid \mathbf{X}, T > t) = \frac{\exp\{-vH(t \mid \mathbf{X})\} g(v)}{L_V\{H(t \mid \mathbf{X})\}}. \tag{2.17}$$

Consequently,

$$\mathbb{E}(V \mid \mathbf{X}, T > t) = -\frac{L_V'\{H(t \mid \mathbf{X})\}}{L_V\{H(t \mid \mathbf{X})\}} = \frac{D(t, \mathbf{X})}{\lambda(\alpha)}, \tag{2.18}$$

where $D(t, \mathbf{X}) = \psi\{\alpha + q(t, \mathbf{X})\} - \psi\{q(t, \mathbf{X})\}$. For an individual who experiences the event at time t, the conditional event density under the proportional hazards formulation contains an additional factor v. Consequently, after cancellation of terms that do not depend on v, the posterior frailty density is

$$g(v \mid \mathbf{X}, T = t) = \frac{v \exp\{-vH(t \mid \mathbf{X})\}g(v)}{-L'_V\{H(t \mid \mathbf{X})\}}. \tag{2.19}$$

Thus, unlike the conditional distribution among survivors, the conditional frailty distribution for an observed failure is not, in general, a simple transformation of a beta distribution. To obtain its conditional mean, define $D(t, \mathbf{X}) = \psi(\alpha + q(t, \mathbf{X})) - \psi(q(t, \mathbf{X}))$. Then

$$\mathbb{E}(V \mid \mathbf{X}, T = t) = \frac{L''_V\{H(t \mid \mathbf{X})\}}{-L'_V\{H(t \mid \mathbf{X})\}}, \tag{2.20}$$

and, using the first and second derivatives of the beta function,

$$\mathbb{E}(V \mid \mathbf{X}, T = t) = \frac{D^2(t, \mathbf{X}) + \psi_1(q(t, \mathbf{X})) - \psi_1(\alpha + q(t, \mathbf{X}))}{\lambda(\alpha)D(t, \mathbf{X})}, \tag{2.21}$$

where $\psi_1(\cdot)$ denotes the trigamma function. Equations (2.18) and (2.21) provide closed-form posterior means for the proportional hazards specification. Let $\widehat{\alpha}$ and $\widehat{H}(t_i \mid \mathbf{X}_i)$ denote the maximum likelihood estimates of the corresponding model quantities, and define

$$\widehat{\lambda} = \psi(\widehat{\alpha} + 1) - \psi(1),\ \widehat{q_i} = 1 + \frac{\widehat{H}(t_i \mid \mathbf{X}_i)}{\widehat{\lambda}},\ \text{and}\ \widehat{D_i} = \psi(\widehat{\alpha} + \widehat{q_i}) - \psi(\widehat{q_i})\,. \tag{2.22}$$

Assuming that $\delta_i = 1$ denotes an observed event and $\delta_i = 0$ a right-censored observation, the empirical Bayes predictor under the proportional hazards specification is

$$\widehat{V_i} = \begin{cases} \dfrac{\widehat{D_i}^2 + \psi_1(\widehat{q_i}) - \psi_1(\widehat{\alpha} + \widehat{q_i})}{\widehat{\lambda}\widehat{D_i}}, & \delta_i = 1, \\ \dfrac{\widehat{D_i}}{\widehat{\lambda}}, & \delta_i = 0. \end{cases} \tag{2.23}$$

It is important to distinguish the individual frailty formulation considered here from the conventional shared-frailty framework. In a shared-frailty model, two or more individuals or repeated event times within the same cluster share a common latent random effect, thereby inducing within-cluster dependence. In the present model, by contrast, each subject has an individual frailty V_i, with $V_1, \ldots, V_n$ assumed to be independent and identically distributed from the proposed EE frailty distribution. Consequently, the frailty component does not induce dependence between different subjects. Because each individual contributes only one possibly censored survival time, the subject-specific frailty V_i is not identified from that observation alone. Rather, the distribution of the latent heterogeneity is identified at the population level through the marginal survival likelihood under the assumed parametric model. In particular, identification relies on specifying both the conditional survival model and the frailty distribution, together with the normalization $\mathbb{E}(V) = 1$, which separates the overall scale of the baseline survival process from the mean frailty effect. The frailty is also assumed

to be independent of the observed covariates, so that its variation represents residual heterogeneity remaining after conditioning on the measured predictors.

Accordingly, Var(V) should be interpreted as a population-level measure of residual unobserved heterogeneity rather than as evidence that an individual latent effect can be precisely recovered for each subject. Subject-specific empirical Bayes estimates are posterior predictions under the fitted parametric model and, with only one survival outcome per subject, are necessarily subject to substantial shrinkage toward the population frailty distribution. For the log-normal accelerated failure time specification considered in the simulation study, the frailty enters the conditional location of log-survival time rather than multiplying the hazard. Therefore, the proportional hazards expressions above do not apply directly. In this case, the posterior mean is obtained from the general individual likelihood contribution. Specifically,

$$\mathbb{E}(V \mid t_i, \delta_i, \mathbf{X}_i) = \frac{\displaystyle\int_0^\infty v \left\{f(t_i \mid v, \mathbf{X}_i)\right\}^{\delta_i} \left\{S(t_i \mid v, \mathbf{X}_i)\right\}^{1-\delta_i} g(v)\, dv}{\displaystyle\int_0^\infty \left\{f(t_i \mid v, \mathbf{X}_i)\right\}^{\delta_i} \left\{S(t_i \mid v, \mathbf{X}_i)\right\}^{1-\delta_i} g(v)\, dv}. \tag{2.24}$$

For the log-normal model used here, $\log(T_i \mid V_i = v, \mathbf{X}_i) = \mu + \mathbf{X}_i^\top \boldsymbol{\beta} - \log(v) + \sigma Z_i,\ Z_i \sim N(0,1)$, and the integrals in (2.24) are evaluated numerically. This formulation is also applicable whenever a closed-form posterior mean is unavailable. The resulting empirical Bayes predictions are posterior means and therefore provide subject-specific summaries of latent heterogeneity conditional on the observed survival information and covariates. Among otherwise comparable individuals, larger predicted frailty values indicate greater residual heterogeneity associated with the event process. These predictions should nevertheless be interpreted with caution. In the present setting, each subject contributes a single, possibly censored, survival outcome rather than repeated events or multiple observations within a shared cluster. Consequently, the information available for estimating an individual latent effect is limited, and the empirical Bayes predictions are naturally shrunk toward the population frailty distribution. They should therefore be interpreted as model-based posterior summaries of residual heterogeneity rather than as precisely identified individual-specific risk parameters.

3. Inference

The inferential procedure depends on the regression formulation described in Section 2. Under the multiplicative-hazard formulation, and particularly under the proportional hazards specification, the closed-form Laplace transform of the EE frailty leads to an explicit marginal likelihood. For the log-normal AFT specification, by contrast, the marginal likelihood is obtained by numerical integration over the frailty distribution.

3.1. Inference under the proportional hazards formulation

Let $\boldsymbol{\Omega} = (\alpha, \Theta^\top, \boldsymbol{\beta}^\top)^\top$, where α denotes the EE frailty parameter, Θ contains the parameters of the baseline hazard, and $\boldsymbol{\beta}$ denotes the regression coefficients. Under proportional hazards, define $H_i = H_0(t_i; \Theta)\exp(\mathbf{X}_i^\top \boldsymbol{\beta}), h_i = h_0(t_i; \Theta)\exp(\mathbf{X}_i^\top \boldsymbol{\beta})$, and let $\lambda(\alpha) = \psi(\alpha + 1) - \psi(1), q_i = 1 + \frac{H_i}{\lambda(\alpha)}$. Furthermore, define $D_i = \psi(\alpha + q_i) - \psi(q_i)$. For a sample $(T_i, \delta_i, \mathbf{X}_i^\top)$, $i = 1, \ldots, n$, the marginal likelihood is

$$L_{\mathrm{PH}}(\boldsymbol{\Omega}) = \prod_{i=1}^{n} f_m(t_i \mid \mathbf{X}_i)^{\delta_i} S_m(t_i \mid \mathbf{X}_i)^{1-\delta_i}, \tag{3.1}$$

and the corresponding log-likelihood can be written compactly as

$$\ell_{\mathrm{PH}}(\boldsymbol{\Omega}) = \sum_{i=1}^{n} \delta_i \left[\log h_i - \log\{\lambda(\alpha)\} + \log D_i\right] + \sum_{i=1}^{n} \left[\log(\alpha) + \log B(\alpha, q_i)\right]. \tag{3.2}$$

The maximum likelihood estimator $\widehat{\boldsymbol{\Omega}}$ is obtained by numerical maximization of (3.2). The score vector and observed information matrix are defined as

$$U(\boldsymbol{\Omega}) = \frac{\partial \ell_{\mathrm{PH}}(\boldsymbol{\Omega})}{\partial \boldsymbol{\Omega}}, \qquad J(\boldsymbol{\Omega}) = -\frac{\partial^2 \ell_{\mathrm{PH}}(\boldsymbol{\Omega})}{\partial \boldsymbol{\Omega} \partial \boldsymbol{\Omega}^{\top}}. \tag{3.3}$$

Analytical expressions for these quantities under the proportional hazards formulation are provided in Appendix B. In practical computation, they may also be evaluated numerically.

3.2. Inference under the log-normal AFT formulation

For the log-normal AFT model, let $\boldsymbol{\Omega}_A = (\alpha, \mu, \sigma, \boldsymbol{\beta}^{\top})^{\top}$. Using the conditional density and survival functions in (2.11), the individual marginal likelihood contribution is

$$m_i(\boldsymbol{\Omega}_A) = \int_0^{\infty} \left\{\frac{\phi\{z_i(v)\}}{\sigma t_i}\right\}^{\delta_i} [1 - \Phi\{z_i(v)\}]^{1-\delta_i} \, g(v; \alpha) \, dv, \tag{3.4}$$

and hence

$$\ell_{\mathrm{AFT}}(\boldsymbol{\Omega}_A) = \sum_{i=1}^{n} \log m_i(\boldsymbol{\Omega}_A). \tag{3.5}$$

Unlike the proportional hazards case, the integration in (3.4) does not generally reduce to the Laplace transform of the frailty distribution because v enters the log-normal location through $-\log(v)$. The integrals are therefore evaluated numerically. In the computations reported in this article, Gauss-Laguerre quadrature is used for this purpose. Maximum likelihood estimation proceeds by numerical maximization of (3.5). Standard errors are obtained from the inverse numerically evaluated observed Hessian of the integrated log-likelihood. Thus, the analytical score and information-matrix expressions reported in Appendix B apply only to the proportional hazards formulation and are not used for the log-normal AFT model. For either formulation, provided that the relevant regularity conditions hold away from boundary cases, the maximum likelihood estimator is asymptotically normal. If ϑ_r denotes a generic scalar component of the corresponding parameter vector, an approximate $(1-\gamma)100\%$ confidence interval is obtained as $\widehat{\vartheta}_r \pm z_{1-\gamma/2} \sqrt{\widehat{\mathrm{Var}}(\widehat{\vartheta}_r)}$.

3.3. Test for unobserved heterogeneity

An important question in frailty modeling is whether the inclusion of a frailty component is supported by the data. In the proposed framework, absence of unobserved heterogeneity corresponds to a degenerate frailty distribution at $V = 1$. Since the EE frailty distribution is parameterized such that $\mathbb{E}(V) = 1$, this is equivalent to $\mathrm{Var}(V) = 0$. For the standardized EE frailty distribution, the variance is

$$\sigma_V^2(\alpha) = \mathrm{Var}(V) = \frac{\psi_1(1) - \psi_1(\alpha+1)}{\{\psi(\alpha+1) - \psi(1)\}^2}, \tag{3.6}$$

where $\psi_1(\cdot)$ denotes the trigamma function. Notice that, under the original parameterization, absence of frailty is attained only in the limit $\alpha \to \infty$. Indeed, using $\psi(\alpha+1) - \psi(1) = \log(\alpha) + \gamma + o(1)$ and $\psi_1(\alpha+1) \to 0$, it follows that

$$\sigma_V^2(\alpha) = \frac{\pi^2/6 + o(1)}{\{\log(\alpha) + \gamma + o(1)\}^2} \longrightarrow 0, \qquad \alpha \to \infty. \tag{3.7}$$

Therefore, rather than formulating the likelihood-ratio test directly in terms of α, we use $\theta = \sigma_V^2 = \mathrm{Var}(V)$ as the local dispersion parameter. The hypotheses of interest can then be written as $H_0 : \theta = 0$ versus $H_1 : \theta > 0$. Under this parameterization, the null hypothesis lies on the finite boundary of the parameter space $\theta \geq 0$. The appropriateness of this boundary parameterization can also be seen from the local behavior of the marginal likelihood. Since $\mathbb{E}(V) = 1$, write $V = 1 + \varepsilon$, where $\mathbb{E}(\varepsilon) = 0$ and $\mathbb{E}(\varepsilon^2) = \theta$. For the EE frailty distribution,

$$\mathbb{E}\{(V-1)^3\} = \frac{\psi_2(\alpha+1) - \psi_2(1)}{\{\psi(\alpha+1) - \psi(1)\}^3} = O(\theta^{3/2}), \qquad \theta \to 0, \tag{3.8}$$

where $\psi_2(\cdot)$ denotes the polygamma function of order two. Consequently, for a sufficiently smooth individual conditional likelihood contribution $m_i(v)$, a Taylor expansion around $v = 1$ gives

$$\mathbb{E}_\theta\{m_i(V)\} = m_i(1) + \frac{\theta}{2} m_i''(1) + o(\theta), \qquad \theta \to 0. \tag{3.9}$$

Thus, under the usual smoothness and integrability conditions, the marginal likelihood is locally differentiable with respect to the variance parameter at $\theta = 0$. To assess the presence of unobserved heterogeneity, we consider the likelihood-ratio statistic

$$RV = -2\log\left(\frac{L(\widehat{\Theta}^*, \widehat{\boldsymbol{\beta}}^*)}{L(\widehat{\Theta}, \widehat{\boldsymbol{\beta}}, \widehat{\alpha})}\right) = -2\Big[\ell(\widehat{\Theta}^*, \widehat{\boldsymbol{\beta}}^*) - \ell(\widehat{\Theta}, \widehat{\boldsymbol{\beta}}, \widehat{\alpha})\Big], \tag{3.10}$$

where $L(\widehat{\Theta}^*, \widehat{\boldsymbol{\beta}}^*)$ denotes the maximized likelihood under the model without frailty, that is, $V_i = 1$, $i = 1, \ldots, n$, whereas $L(\widehat{\Theta}, \widehat{\boldsymbol{\beta}}, \widehat{\alpha})$ denotes the maximized likelihood under the EE frailty model. Although estimation under the alternative is performed using the original parameter α, the likelihood-ratio statistic is unchanged by the one-to-one reparameterization through the frailty variance for finite α. The variance parameterization is used to characterize the limiting null hypothesis as $\theta \downarrow 0$. Under the usual regularity conditions for the remaining model parameters, local identifiability of the variance component, and positive information for θ at the null, the only nonstandard feature of the test is that $\theta = 0$ lies on the boundary of the parameter space [16]. Hence, the likelihood-ratio statistic has the one-sided boundary distribution $RV \xrightarrow{d} \frac{1}{2}\chi_0^2 + \frac{1}{2}\chi_1^2$, where χ_0^2 denotes a point mass at zero and χ_1^2 is a chi-square distribution with one degree of freedom. Accordingly, for an observed value $RV > 0$, the corresponding asymptotic p-value is $p = \frac{1}{2}\Pr\left\{\chi_1^2 \geq RV\right\}$. This formulation makes explicit that the boundary argument is applied to the frailty variance parameter rather than directly to the EE shape parameter α, for which the no-frailty hypothesis occurs only at the non-finite limit $\alpha \to \infty$. The

estimated frailty variance should therefore be interpreted as residual population heterogeneity under the assumed survival and frailty models. It may reflect genuinely unmeasured risk factors, but also omitted observed predictors or remaining model misspecification, and should not be interpreted as a directly observed subject-specific risk component.

Particular cases:

- *Weibull PH EE frailty model.* For the Weibull proportional hazards model,

$$h_0(t) = \theta t^{\theta-1}, \qquad H_0(t) = t^{\theta},$$

and therefore

$$h(t \mid \mathbf{X}) = \theta t^{\theta-1} \exp(\mathbf{X}^{\top}\boldsymbol{\beta}), \qquad H(t \mid \mathbf{X}) = t^{\theta} \exp(\mathbf{X}^{\top}\boldsymbol{\beta}).$$

Substitution of these expressions into the multiplicative-hazard EE frailty formulation yields the corresponding closed-form marginal survival, density, hazard, and likelihood functions.

- *Log-normal AFT EE frailty model.* The log-normal model used in the simulation and empirical application is not obtained by substituting a log-normal cumulative hazard into the proportional hazards expressions. Instead, it is defined through

$$\log(T_i \mid V_i = v, \mathbf{X}_i) = \mu + \mathbf{X}_i^{\top}\boldsymbol{\beta} - \log(v) + \sigma Z_i, \qquad Z_i \sim N(0,1).$$

Its marginal density and survival functions are obtained by integrating the corresponding conditional log-normal quantities with respect to the frailty distribution, as described in (2.12)–(3.5). These integrals are evaluated numerically.

4. Simulation study

A Monte Carlo simulation study was conducted to investigate the finite-sample performance of the proposed EE frailty model and to compare it with the classical gamma frailty model under both correct specification and frailty-distribution misspecification. The simulation design follows the general framework commonly adopted in the frailty literature for assessing finite-sample properties under different sample sizes, censoring proportions, levels of heterogeneity, and baseline survival specifications [4, 6, 7].

We considered three baseline survival specifications representing different shapes of the event-time distribution: a Weibull proportional hazards model with shape parameter $k = 0.7$, corresponding to a decreasing baseline hazard; a Weibull proportional hazards model with shape parameter $k = 1.5$, corresponding to an increasing baseline hazard; and a log-normal accelerated failure time model with parameters $\mu = 0$ and $\sigma = 0.6$, producing a non-monotone hazard pattern. The regression structure consisted of a single binary covariate $X \sim$ Bernoulli(0.5) with regression coefficient $\beta = 0.7$.

Independent right censoring was generated from an exponential distribution, with its rate calibrated to produce approximately 0%, 30%, 60%, and 90% censoring. The 90% censoring condition was included to evaluate the behavior of the estimation procedure under a level of censoring at least as severe as that observed in the empirical application, where approximately 84.1% of the observations were right-censored. Five sample sizes were considered, $n \in \{50, 100, 200, 500, 1000\}$, together with two levels of unobserved heterogeneity. For gamma frailty, the variance parameter was set to $\theta \in \{0.281, 0.556\}$, whereas for EE frailty the corresponding shape parameters were $\alpha \in \{5, 2\}$.

These values were selected so that the two frailty distributions had the same target frailty variances, Var(V)=0.281 and Var(V) = 0.556. For each scenario, 1000 Monte Carlo samples were generated. Two frailty data-generating mechanisms were considered: gamma frailty and EE frailty. Each generated data set was then fitted with both frailty specifications. Consequently, four data-generating/fitted-model combinations were examined:

$$\text{Gamma} \to \text{Gamma}, \qquad \text{Gamma} \to \text{EE}, \qquad \text{EE} \to \text{EE}, \qquad \text{EE} \to \text{Gamma}.$$

The Gamma→Gamma and EE→EE combinations represent correctly specified models, whereas Gamma→EE and EE→Gamma constitute frailty-distribution misspecification scenarios. The same baseline survival specifications, sample sizes, censoring levels, regression parameter, and target frailty variances were retained across the four combinations. Matching the frailty distributions on Var(V) ensured that differences between the fitted models were not driven simply by different amounts of latent heterogeneity. This cross-fitting design allows us to assess the consequences of frailty-distribution misspecification and the sensitivity of parameter estimation, numerical convergence, and subject-specific frailty prediction to the assumed frailty family.

Parameter estimation was performed by maximum likelihood using numerical optimization. Only solutions satisfying the strict convergence criterion were retained for estimation-performance summaries. Convergence required successful numerical optimization, a maximum absolute score component smaller than 10^{-4}, and the additional numerical checks described below.

The performance of the regression estimator was assessed through its empirical bias, empirical standard deviation, and root mean squared error (RMSE). The same measures were computed for the frailty variance estimator Var(V). In addition, the ability of each model to recover the latent frailty effects was evaluated using empirical Bayes predictions. For each simulated individual, the posterior mean of the frailty was computed and summarized by the mean predicted frailty; the root mean squared prediction error, $RMSE(\widehat{V}, V)$; and Spearman's rank correlation between the predicted and true frailties. This design allows the proposed EE frailty model and the classical gamma frailty model to be compared under different survival-model specifications, sample sizes, censoring proportions, and heterogeneity levels in terms of parameter estimation and prediction of individual frailty effects. Bias, SD, and RMSE were computed from converged replications only.

Although empirical coverage probabilities would provide an additional assessment of the Hessian-based confidence intervals developed in Section 3, a systematic coverage study was not undertaken as part of the present simulation design. Such an assessment would require replication-specific valid observed-information matrices across the different baseline models, heterogeneity levels, sample sizes, and censoring conditions. Accordingly, the confidence-interval results developed in Section 3 should be interpreted as asymptotic, and a systematic investigation of their finite-sample coverage, particularly under severe censoring, is left for future research.

4.1. Discussion of the simulation results

We summarize the finite-sample performance of the proposed maximum likelihood estimation procedure in Figures 1–3 and Tables 5–10. To facilitate the presentation of the simulation results, the figures are retained in the main text because they provide a visual summary of the principal performance measures, whereas the more detailed numerical results, including bias and convergence rates, are reported in the Appendix.

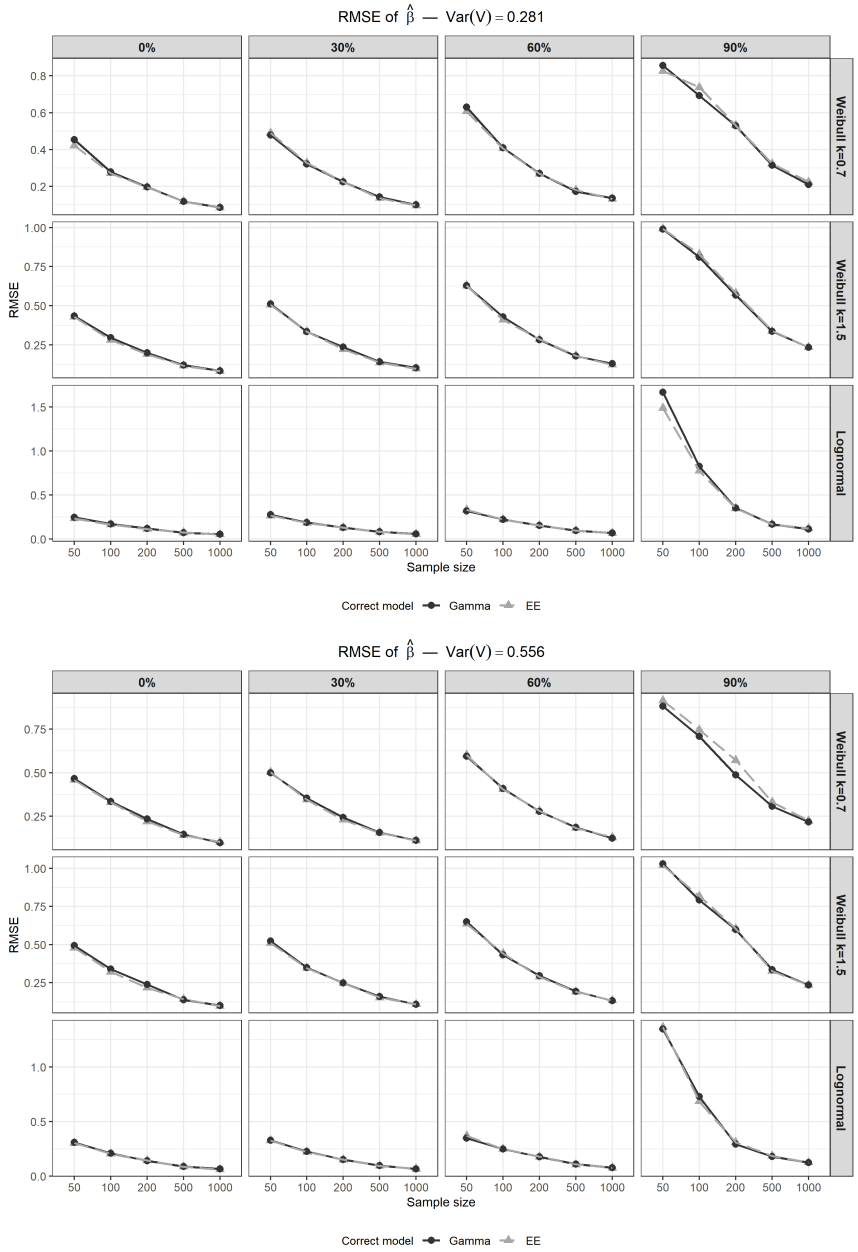


Figure 1. RMSE of the regression parameter estimates.

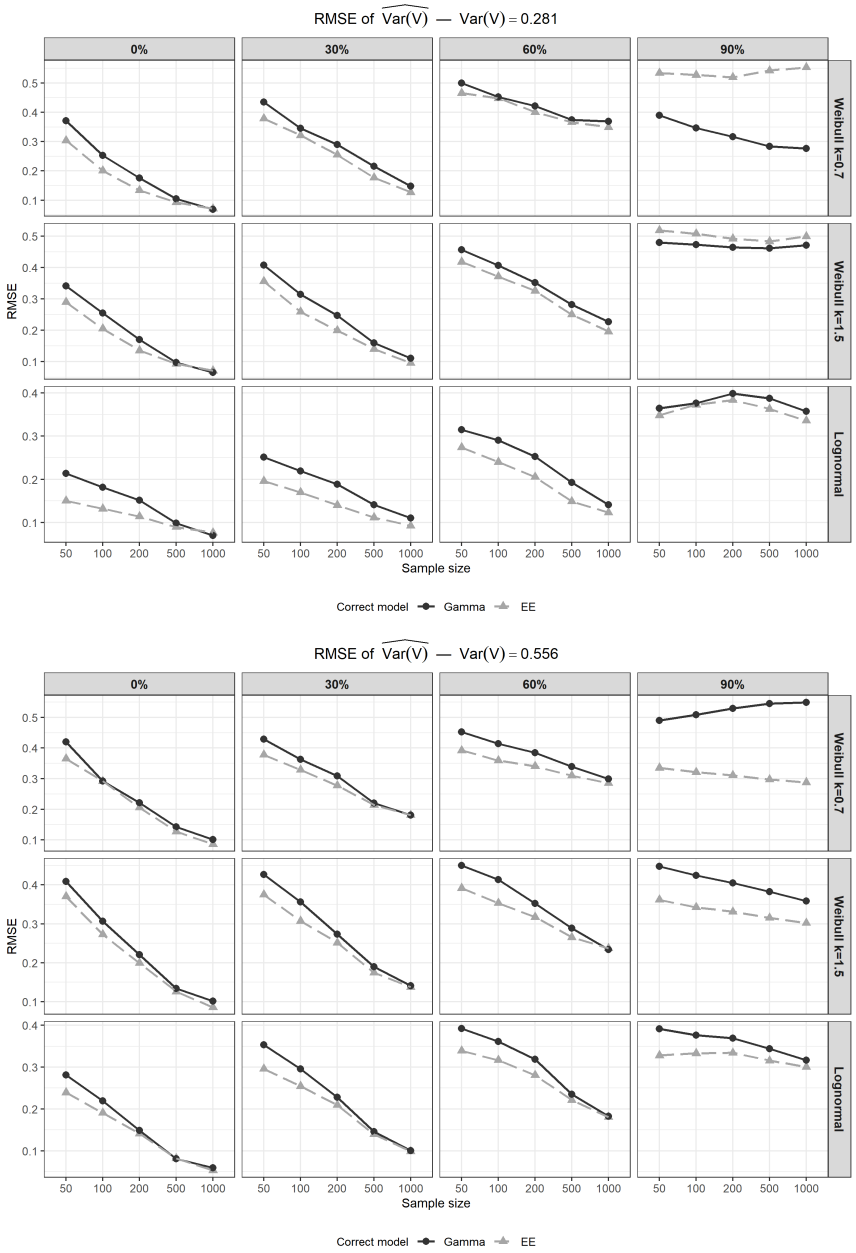


Figure 2. RMSE of the frailty variance estimates.

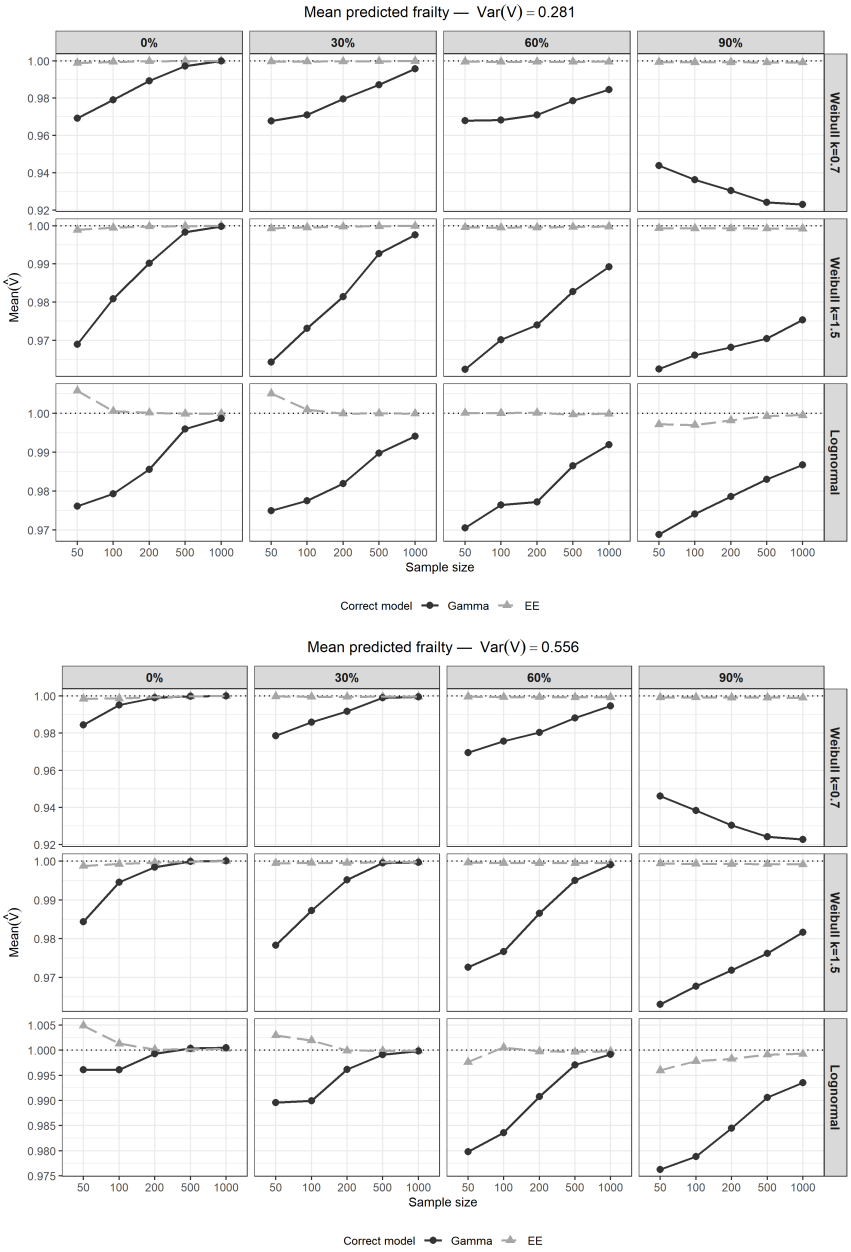


Figure 3. Individual frailty predictions.

A first important aspect is the numerical stability of the estimation procedure. Convergence was generally very high under 0%, 30% and 60% censoring, whereas more noticeable numerical difficulties appeared under the severe 90% censoring scenarios. The latter condition was included as a stress test motivated by the high censoring proportion observed in the empirical application. As expected, the largest deterioration occurred for the smallest sample sizes, reflecting the limited amount of event information available under extremely heavy censoring. For moderate and large samples, numerical performance improved substantially, although the 90% condition remained more demanding than the lower-censoring scenarios. This severe-censoring scenario should be interpreted as a stress test rather

than as an exact replication of the empirical censoring mechanism. Nevertheless, it provides direct information on the behavior of the estimators under a censoring intensity comparable to, and slightly more extreme than, that observed in the tuberculosis application.

The results regarding the estimation of the regression coefficients, as illustrated by Figure 1, show the expected improvement in estimation accuracy as the sample size increases. For both frailty distributions, the absolute bias remained close to zero, whereas the empirical standard deviation and RMSE decreased as the sample size increased. As expected, increasing the censoring proportion produced greater estimation variability, particularly for small sample sizes, although this effect became progressively less important for moderate and large samples.

Before examining the remaining estimation results in greater detail, we assessed the numerical stability of the estimation procedure. Table 1 summarizes the strict convergence rates and the maximum proportion of discarded replications across baseline models, frailty distributions, and censoring levels. Bias, empirical standard deviation, and RMSE reported in the simulation tables were calculated from replications satisfying the strict convergence criterion. The discarded proportions are therefore reported explicitly to quantify the amount of simulation information excluded from these performance measures.

Table 1. Summary of strict convergence and discarded replications across the simulation study.

Baseline	Frailty	Cens. (%)	Mean strict conv. (%)	Min strict conv. (%)	Max discarded (%)
Weibull ($k = 0.7$)	Gamma	0	100.00	100.00	0.00
		30	100.00	100.00	0.00
		60	100.00	100.00	0.00
		90	94.91	78.00	22.00
	EE	0	99.95	99.60	0.40
		30	99.43	98.60	1.40
		60	95.26	93.30	6.70
		90	92.79	75.90	24.10
Weibull ($k = 1.5$)	Gamma	0	100.00	100.00	0.00
		30	100.00	100.00	0.00
		60	100.00	100.00	0.00
		90	95.47	80.30	19.70
	EE	0	99.98	99.90	0.10
		30	99.58	98.70	1.30
		60	97.57	96.30	3.70
		90	87.77	73.00	27.00
Lognormal	Gamma	0	100.00	100.00	0.00
		30	100.00	100.00	0.00
		60	99.95	99.70	0.30
		90	91.18	65.50	34.50
	EE	0	100.00	100.00	0.00
		30	100.00	100.00	0.00
		60	99.94	99.70	0.30
		90	88.37	61.70	38.30

The convergence results indicate generally satisfactory numerical performance up to 60% censoring,

although convergence was not uniformly close to 100% across all settings. Under gamma frailty, strict convergence was essentially 100% up to 60% censoring. Under EE frailty, convergence remained high but showed a modest deterioration as censoring increased. At 60% censoring, the lowest setting-specific strict convergence rate was 93.3%, corresponding to a maximum discarded proportion of 6.7%.

The severe 90% censoring scenarios were substantially more challenging. Depending on the survival specification and frailty distribution, the maximum discarded proportion ranged from 19.7% to 38.3%. These results indicate that the estimation procedure performs reliably under low and moderate censoring, while numerical difficulties become more pronounced under very heavy censoring, particularly for smaller sample sizes.

The estimation of the frailty variance was substantially more challenging than that of the regression coefficient, particularly as the amount of censoring increased. Under no or moderate censoring, both frailty specifications generally showed decreasing variability and improved estimation as the sample size increased. At 60% censoring, however, some persistent bias was already evident in the heterogeneity parameter despite the generally satisfactory numerical convergence.

The 90% censoring scenarios revealed a more important limitation. For several settings, particularly under the Weibull PH specifications, increasing the sample size reduced sampling variability without eliminating substantial bias in $\widehat{\mathrm{Var}}(V)$. Consequently, RMSE did not decrease monotonically in all scenarios. This behavior indicates that an increased nominal sample size cannot fully compensate for the limited event information available under extreme censoring. Neither frailty distribution showed uniform superiority: Relative performance depended on the baseline model, heterogeneity level, and censoring proportion. These results therefore support the EE model as a competitive alternative to gamma frailty under low and moderate censoring, while also demonstrating that estimation of latent heterogeneity can become unreliable under extremely sparse event information.

The prediction of individual frailties is illustrated in Figure 3. As expected, the average predicted frailty converged to its theoretical mean, $E(V) = 1$, whereas the prediction RMSE decreased steadily as the sample size increased. These improvements were more gradual than those observed for the regression and heterogeneity parameters, reflecting the intrinsic difficulty of estimating subject-specific random effects from limited individual follow-up information. Taken together, the simulation study provides evidence of satisfactory finite-sample estimation of the regression effect under low and moderate censoring, while showing that estimation of the frailty variance becomes substantially more difficult as event information decreases. Numerical stability was generally high up to 60% censoring, whereas the severe 90% censoring scenarios revealed important limitations in both convergence and heterogeneity estimation. These findings reinforce the need for cautious inference on the frailty component when censoring is extreme.

These findings support the proposed EE frailty distribution as a competitive alternative to the classical gamma frailty for modeling unobserved heterogeneity in survival data. The simulation results complement recent developments in alternative frailty distributions reported by [8–10]. Similar to these proposals, the EE frailty exhibits stable maximum likelihood estimation and satisfactory finite-sample performance over a broad range of simulation settings. However, the present model is constructed from a different distributional family and provides an additional flexible alternative for modeling latent heterogeneity. The similar qualitative patterns observed across the Weibull PH and log-normal AFT settings further indicate that the performance of the proposed frailty specification is not restricted to a single survival model formulation. The EE frailty therefore contributes to the growing literature on

flexible frailty distributions by combining a positive random effect, a closed-form Laplace transform in the proportional hazards setting, and competitive finite-sample performance relative to the classical gamma frailty.

4.2. Sensitivity to frailty-distribution misspecification

To assess the robustness of the estimation procedure to misspecification of the frailty distribution, we conducted a cross-fitting experiment in which gamma-generated samples were fitted using the EE frailty model and EE-generated samples were fitted using the gamma frailty model. The same baseline survival specifications, sample sizes, censoring levels, regression parameter, and target frailty variances considered under correct specification were retained. Because the gamma and EE distributions were matched through $\mathrm{Var}(V)$, differences between the cross-fitted models reflect distributional misspecification rather than differences in the overall magnitude of latent heterogeneity.

The analysis focused on the sensitivity of the regression coefficient, frailty variance, numerical convergence, and subject-specific frailty prediction to the assumed frailty family. For each direction of misspecification and censoring level, the summary statistics in Table 2 represent 30 simulation settings obtained from the combination of three baseline specifications, five sample sizes, and two frailty-variance levels.

Table 2. Sensitivity to frailty-distribution misspecification. Results are summarized across the 30 simulation settings corresponding to each direction of misspecification and censoring level. Bias, RMSE, and Spearman correlation entries are medians across simulation settings. For strict convergence, the median rate is reported first and the minimum setting-specific rate is shown in brackets.

True → fitted	Censoring	Conv. rate	$\lvert\mathrm{Bias}(\widehat{\beta})\rvert$	$\mathrm{RMSE}(\widehat{\beta})$	$\lvert\mathrm{Bias}(\widehat{\mathrm{Var}}(V))\rvert$	$\mathrm{RMSE}(\widehat{\mathrm{Var}}(V))$	Spearman ρ
EE → Gamma	0%	1.000 [1.000]	0.005	0.177	0.060	0.175	0.542
EE → Gamma	30%	1.000 [1.000]	0.006	0.201	0.049	0.239	0.492
EE → Gamma	60%	1.000 [0.997]	0.011	0.245	0.040	0.342	0.387
EE → Gamma	90%	0.998 [0.657]	0.032	0.521	0.135	0.391	0.149
Gamma → EE	0%	1.000 [0.996]	0.005	0.183	0.045	0.154	0.551
Gamma → EE	30%	1.000 [0.979]	0.013	0.205	0.059	0.222	0.499
Gamma → EE	60%	0.984 [0.948]	0.019	0.246	0.093	0.315	0.397
Gamma → EE	90%	0.936 [0.611]	0.045	0.558	0.210	0.354	0.154

The cross-fitting experiment indicates that estimation of the regression coefficient is relatively robust to moderate misspecification of the frailty distribution. Under censoring levels up to 60%, the median absolute bias of $\widehat{\beta}$ remained small in both directions of misspecification, ranging from 0.005 to 0.019. The corresponding RMSE increased gradually with censoring but remained similar whether EE data were fitted using gamma frailty or gamma data were fitted using EE frailty. This suggests that, for estimation of the regression effect, the two frailty distributions can provide reasonably similar marginal behavior when their heterogeneity levels are comparable. Estimation of the frailty variance was more sensitive to distributional misspecification. Although median absolute bias remained moderate under low and intermediate censoring, the RMSE of $\widehat{\mathrm{Var}}(V)$ increased as censoring became more severe. The effect was particularly evident under 90% censoring, where the median absolute bias reached 0.135 for EE data fitted with a gamma frailty and 0.210 for gamma data fitted with an EE frailty. Thus, recovery

of the magnitude of latent heterogeneity is more dependent on the assumed frailty distribution than estimation of the regression coefficient.

A similar pattern was observed for the subject-specific frailty predictions. The median Spearman correlation between the true and predicted frailties was approximately 0.54–0.55 in the absence of censoring and decreased progressively as censoring increased. Under 90% censoring, the median correlations were only 0.149 and 0.154 for the two directions of misspecification. This deterioration reflects the substantial loss of individual-level information available for recovering the latent frailty under severe censoring and reinforces the need to interpret individual empirical Bayes frailty predictions cautiously.

Numerical performance was generally satisfactory under censoring levels up to 60%. Median strict convergence rates were essentially one for EE data fitted with gamma frailty and remained at least 0.984 when gamma data were fitted with EE frailty. Under 90% censoring, convergence became more scenario-dependent, particularly for the gamma-to-EE fit, for which the median strict convergence rate decreased to 0.936 and the minimum rate across simulation settings was 0.611. Overall, the misspecification experiment shows that the gamma and EE frailty models are relatively interchangeable for estimation of the regression effect under low to moderate censoring, whereas estimation and prediction of the latent heterogeneity are substantially more sensitive to both the assumed frailty distribution and the amount of censoring.

5. Application

The proposed methodology was illustrated using surveillance data on pulmonary tuberculosis reported to the Colombian National Public Health Surveillance System (SIVIGILA) [17]. The analysis was based on records from the 2025 surveillance database. Individuals were eligible if they had a recorded hospitalization date and were classified as hospitalized when the hospitalization indicator was available. Records were excluded when the hospitalization-to-end-of-follow-up time could not be determined, when the resulting follow-up time was negative, or when information on age or sex was missing. Thus, the analysis was based on complete cases for the variables required by the survival model.

The survival outcome was defined as the time, in days, from hospitalization to death. A death was considered an observed event when a valid date of death was available on or after the hospitalization date. For individuals without a recorded death, follow-up was right-censored at the latest administrative date available in the individual record among the corresponding notification, adjustment, and record-closing dates. No common administrative censoring date was imposed; rather, the end of follow-up was determined individually from the latest administrative date available in each record. Observed survival times equal to zero, corresponding to an event or censoring on the day of hospitalization, were set to 0.5 days to permit fitting of continuous survival models.

After application of these eligibility and data-quality criteria, the final analytical sample consisted of $n = 9594$ individuals, of whom 1522 (15.9%) experienced the event and 8072 (84.1%) were right-censored. The regression structure included age and sex as explanatory variables. Age was expressed in years and standardized before model fitting by subtracting its sample mean and dividing by its sample standard deviation, whereas sex was represented by a binary indicator, with female as the reference category. The analytical sample included 6499 males (67.7%) and 3095 females (32.3%). The data

were obtained from the SIVIGILA online platform through an authenticated access procedure. Access to the database required logging into the platform, indicating the purpose of the data request, and providing a valid e-mail address before download. The analysis was based on secondary surveillance records and did not involve direct contact with participants or the prospective collection of personal information. No additional individual-level data were collected for this study. Model comparison was based on the Akaike information criterion (AIC), its small-sample correction (AICc), and the Hannan-Quinn information criterion (HQIC), defined as

$$AIC = -2\ell(\widehat{\boldsymbol{\theta}}) + 2k, AIC_c = AIC + \frac{2k(k+1)}{n-k-1}, HQIC = -2\ell(\widehat{\boldsymbol{\theta}}) + 2k\log(\log n). \tag{5.1}$$

Smaller values of these criteria indicate a better compromise between goodness of fit and model complexity.

The results in Table 3 show substantial differences between the Weibull and log-normal specifications. The Weibull model without frailty provided the poorest fit according to all three information criteria. Introducing a frailty component substantially improved the Weibull model, reducing the AIC by more than 150 units. The log-normal specifications nevertheless provided a better fit than their corresponding Weibull counterparts. The inclusion of a frailty component also improved the log-normal model. Relative to the log-normal model without frailty, the AIC decreased from 19837.30 to 19820.88 under gamma frailty and to 19820.60 under EE frailty. Similar conclusions were obtained from AICc and HQIC. Formal likelihood-ratio tests also provided strong evidence in favor of including a frailty component. Comparing each log-normal frailty model with the corresponding model without frailty yielded $RV = 18.42$ for gamma frailty and $RV = 18.70$ for EE frailty. Using the boundary distribution $\frac{1}{2}\chi_0^2 + \frac{1}{2}\chi_1^2$, the corresponding p-values were 8.86×10^{-6} and 7.65×10^{-6}, respectively. Thus, both frailty specifications provide strong evidence of residual heterogeneity after adjustment for the observed covariates.

Table 3. Comparison of model fits for the pulmonary tuberculosis data.

Model	Log-likelihood	AIC	AICc	HQIC
Log-normal + EE frailty	−9905.30	19820.60	19820.61	19832.76
Log-normal + Gamma frailty	−9905.44	19820.88	19820.88	19833.04
Log-normal	−9914.65	19837.30	19837.30	19847.02
Weibull + Gamma frailty	−9915.32	19840.63	19840.64	19852.79
Weibull + EE frailty	−9916.00	19842.00	19842.00	19854.16
Weibull	−9993.80	19995.60	19995.61	20005.33

Among the six specifications, the log-normal model with EE frailty had the largest maximized log-likelihood and the numerically smallest AIC, AICc, and HQIC. However, its AIC differed from that of the corresponding gamma frailty model by only 0.28 units. Such a small difference does not provide meaningful evidence favoring one frailty distribution over the other. Rather, the two log-normal frailty specifications provide essentially equivalent empirical fit to these data. Therefore, the application supports the proposed EE frailty as a competitive alternative to the classical gamma frailty, rather than demonstrating empirical superiority of one specification over the other.

Table 4 presents the parameter estimates for the three log-normal specifications, with standard errors reported in parentheses. The estimated effect of standardized age was negative and highly stable across

the three models, ranging from −0.795 to −0.792. Under the adopted log-normal AFT specification, the estimate for the frailty models corresponds to a time ratio of approximately $\exp(-0.792) = 0.453$, indicating shorter survival times following hospitalization for an increase of one standard deviation in age.

Table 4. Parameter estimates for the log-normal models fitted to the pulmonary tuberculosis data.

Parameter	Log-normal	Log-normal + Gamma	Log-normal + EE
μ	7.126 (0.113)	6.690 (0.115)	6.686 (0.115)
σ	2.985 (0.059)	2.819 (0.062)	2.817 (0.062)
Age (standardized)	−0.795 (0.049)	−0.792 (0.049)	−0.792 (0.049)
Male	−0.276 (0.104)	−0.275 (0.104)	−0.275 (0.104)
Var(V)	–	0.831 (0.048)	0.848 (0.043)

Similarly, the coefficient associated with male sex was approximately −0.275, corresponding to a time ratio of $\exp(-0.275) = 0.760$ relative to females. An important feature of these results is the stability of the regression coefficients after introducing unobserved heterogeneity. The estimates of the age and sex effects are virtually unchanged under the gamma and EE frailty specifications. Thus, the substantive conclusions concerning the observed covariates remain essentially unchanged when the gamma frailty distribution is replaced by the EE frailty distribution.

The estimated frailty variances were $\widehat{\text{Var}}(V) = 0.831$ under the gamma model and $\widehat{\text{Var}}(V) = 0.848$ under the EE model. Using the reported standard errors, the corresponding approximate 95% Wald confidence intervals were $(0.737, 0.925)$ and $(0.764, 0.932)$, respectively. Both intervals lie well above zero and are highly overlapping, which is consistent with the likelihood-ratio results and indicates a similar magnitude of residual heterogeneity under the two frailty distributions. Although the EE model produces a slightly larger estimated frailty variance and a slightly smaller associated standard error, these numerical differences are small and should not be interpreted as evidence of superior inferential performance.

It is important, however, to interpret these frailty variances conditionally on the covariates included in the fitted models. The present application adjusts only for age and sex. Consequently, Var(V) should be understood as residual heterogeneity remaining after adjustment for these two observed predictors, rather than as a direct measure of intrinsically unobservable individual risk. Part of the estimated frailty variance may reflect omitted or unavailable measured risk factors, differences in clinical status, treatment, comorbidities, socioeconomic conditions, or other relevant predictors not included in the present analysis, as well as possible remaining model misspecification. The frailty term therefore summarizes residual variation under the assumed model and covariate set, without identifying the specific sources of that heterogeneity.

To complement the global model comparison, model adequacy was also examined using Cox-Snell residuals. Residuals were obtained from the fitted marginal survival distributions, and their Nelson-Aalen cumulative hazard estimates were compared with the unit-slope reference line. Because an overall residual plot may conceal systematic departures within relevant subgroups, the diagnostics were additionally examined after stratification by sex and by age groups. The corresponding diagnostic plots for the log-normal gamma and EE frailty models are shown in Figure 4.

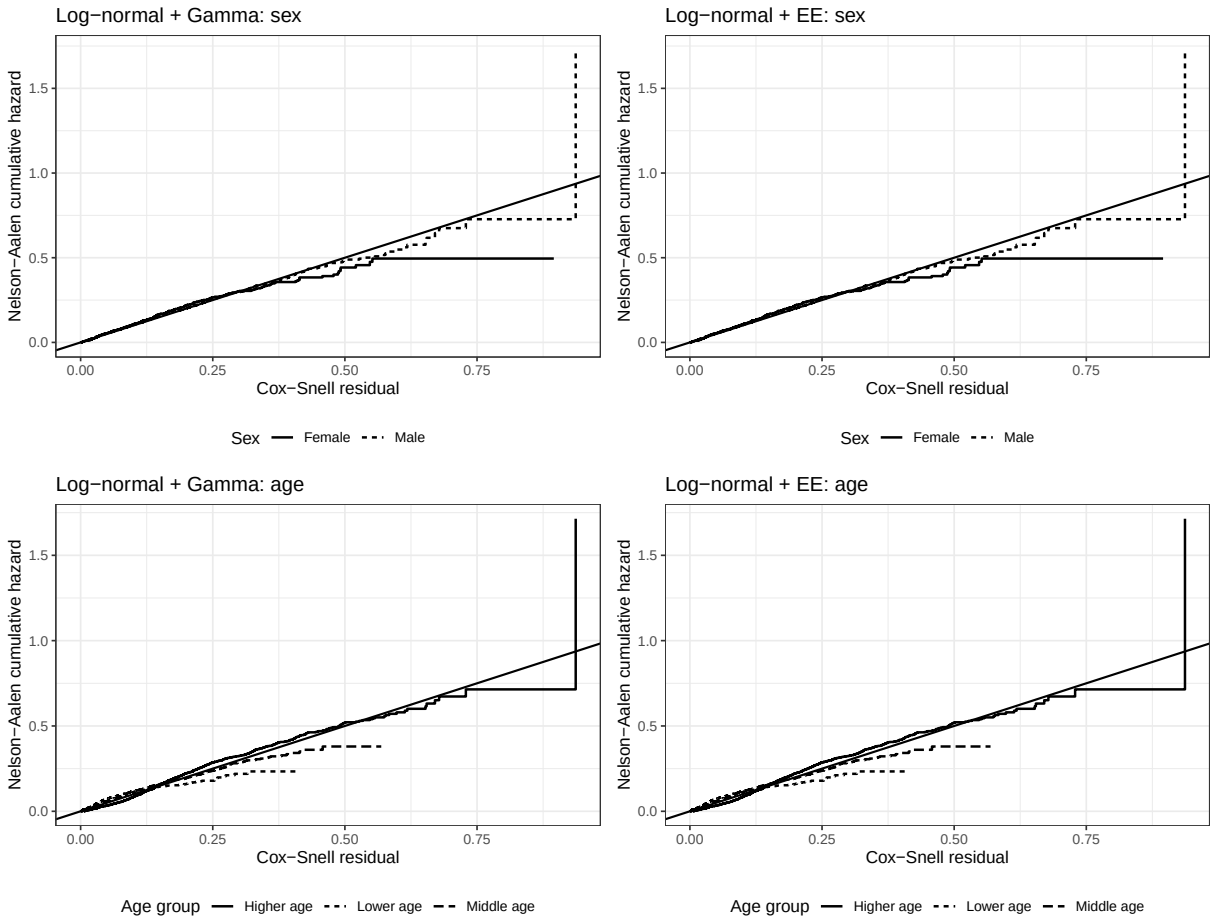


Figure 4. Cox-Snell residual diagnostics for the log-normal gamma and EE frailty models, stratified by sex and age groups. The straight reference line represents the cumulative hazard expected under a unit exponential distribution.

The stratified Cox-Snell residual diagnostics in Figure 4 show broadly similar patterns for the log-normal gamma and EE frailty models. Across sex and age strata, the estimated Nelson-Aalen cumulative hazards follow the unit-slope reference line reasonably well over most of the residual range. Some departures are observed in the extreme right tail, where the number of individuals remaining at risk is necessarily small because of the high censoring proportion. Importantly, no clear systematic difference is apparent between the gamma and EE specifications. These diagnostics are therefore consistent with the likelihood-based results, which indicate that the two frailty models provide essentially equivalent empirical fit.

In addition to the information criteria used for relative model comparison, model adequacy was assessed by comparing the Kaplan-Meier estimator with the corresponding fitted marginal survival functions. This comparison is particularly relevant in the presence of right censoring, since the Kaplan-Meier estimator incorporates information from both observed events and censored observations. The empirical Bayes posterior mean frailty predictions were also examined under the gamma and EE specifications to characterize the subject-specific posterior frailty summaries produced by the two competing frailty models.

Figure 5 complements the information-criterion results. The fitted marginal survival functions provide a direct assessment of the agreement between the parametric models and the Kaplan-Meier estimate while properly accounting for right censoring. In addition, the distributions of the empirical Bayes posterior mean frailty predictions are remarkably similar under the gamma and EE specifications. Their means are approximately 0.999 under both models, with standard deviations of 0.180 and 0.183 for the gamma and EE specifications, respectively. These empirical Bayes predictions are considerably less dispersed than the corresponding fitted population frailty distributions. Indeed, the estimated frailty variances of 0.831 and 0.848 imply population frailty standard deviations of approximately 0.912 and 0.921, respectively, whereas the standard deviations of the posterior mean predictions are only about 0.18.

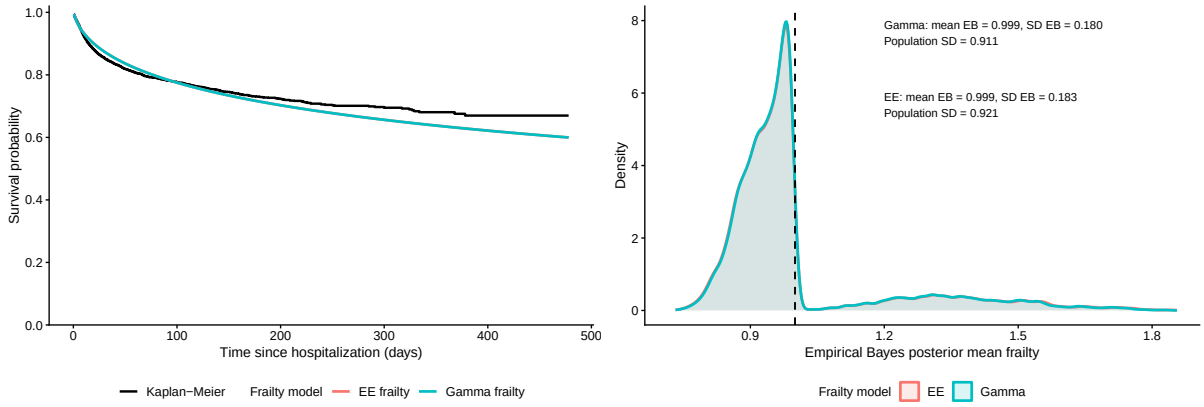


Figure 5. Model adequacy and empirical Bayes frailty predictions for the pulmonary tuberculosis data. Left: fitted marginal survival functions compared with the Kaplan-Meier estimator. Right: distributions of the empirical Bayes posterior mean frailty predictions under the gamma and EE specifications. The concentration of the posterior means around $V = 1$, relative to the substantially larger dispersion implied by the fitted population frailty distributions, illustrates the shrinkage associated with limited subject-specific survival information.

This difference illustrates the substantial shrinkage induced by the limited subject-specific information available in the present application. Because each individual contributes only one possibly censored survival time, the empirical Bayes estimates should not be interpreted as precise measurements of individual latent risk. Rather, they are model-based posterior summaries that combine the individual's observed survival information with the fitted population frailty distribution. Accordingly, relatively large or small predicted frailty values may be useful for describing relative residual heterogeneity within the fitted model, but they should not be interpreted as directly observed or precisely identified subject-specific risk effects.

Overall, the application provides evidence of appreciable residual heterogeneity in the time from hospitalization to death after adjustment for age and sex. Accounting for this heterogeneity improved model fit, particularly under the log-normal specification. The gamma and EE frailty models yielded nearly identical regression effects, comparable estimates of the frailty variance, and very similar empirical Bayes frailty predictions. The estimated frailty component should nevertheless be interpreted as residual heterogeneity conditional on the limited set of observed covariates included in the analysis,

and may partly represent the effects of relevant measured or measurable risk factors that were not available or were not included in the present model. Although the EE model attained marginally smaller information criteria, the differences between the two frailty specifications were modest. Taken together, these results support the proposed EE frailty distribution as a competitive alternative to the classical gamma frailty for modeling residual heterogeneity in survival data.

A natural extension of the proposed framework is its combination with cure-rate models, which would allow residual heterogeneity among susceptible individuals to be considered together with a cured fraction. Such an extension raises additional issues of identifiability and separation between frailty-induced heterogeneity and the cure component. Because these questions require dedicated theoretical and empirical investigation, cure-rate models are not developed in the present study and are left for future research.

6. Conclusions

The proposed EE frailty distribution provides a flexible parametric alternative for modeling residual heterogeneity in survival data. Under the proportional hazards formulation, its closed-form Laplace transform yields explicit marginal survival quantities and facilitates likelihood-based inference. The same standardized frailty distribution can also be incorporated into a log-normal accelerated failure time model, although in that setting marginalization over the frailty distribution is performed numerically. The Monte Carlo study showed generally satisfactory finite-sample estimation of the regression effects under low and moderate censoring, while also revealing greater sensitivity of frailty-variance estimation and numerical convergence under severe censoring. Estimation accuracy generally improved with increasing sample size, although larger samples did not eliminate the difficulties associated with extremely sparse event information in all scenarios. The real-data application further illustrated the practical usefulness of the proposed model. In particular, the log-normal gamma and EE frailty specifications produced essentially equivalent empirical fits, with an AIC difference of only 0.28 units.

Accordingly, the empirical results should not be interpreted as evidence that the EE frailty distribution is superior to the classical gamma frailty. Rather, they support the EE specification as an additional competitive parametric alternative for modeling residual heterogeneity conditional on the observed covariates. As in any frailty analysis, this residual variation may reflect genuinely unmeasured characteristics, omitted observed predictors, or remaining model misspecification and should not be attributed exclusively to intrinsically unobservable individual risk.

Future research may consider extending the proposed frailty distribution to correlated frailty structures for clustered and multistate survival data, as well as investigating Bayesian estimation procedures, semiparametric regression frameworks, and diagnostic tools for assessing the adequacy of the frailty specification. Such developments would further broaden the applicability of the proposed model to more complex survival settings frequently encountered in biomedical and epidemiological studies.

Author contributions

Javier Ramírez-Montoya: Conceptualization, Methodology, Formal analysis, Software, Investigation, Visualization, Writing-original draft, Project administration, Funding acquisition; Guillermo Martínez-Flórez: Conceptualization, Methodology, Validation, Writing-review and editing, Supervision; Rodrigo M. R. de Medeiros: Methodology, Validation, Writing-review and editing.

Use of Generative-AI tools declaration

The authors used AI tools for language editing and to improve the presentation of the manuscript. All scientific content, mathematical derivations, statistical analyses, and conclusions were independently developed and verified by the authors, who assume full responsibility for the work.

Acknowledgments

This research was financially supported by Universidad de Córdoba, Colombia, through the project *Modelamiento de la heterogeneidad no observada* (Project code: FCB-16-25). The authors gratefully acknowledge this support.

Conflict of Interest

The authors declare no conflicts of interest.

References

1. J. W. Vaupel, K. G. Manton, E. Stallard, The impact of heterogeneity in individual frailty on the dynamics of mortality, *Demography*, **16** (1979), 439–454. https://doi.org/10.2307/2061224
2. P. Hougaard, *Analysis of multivariate survival data*, New York: Springer, 2000. https://doi.org/10.1007/978-1-4612-1304-8
3. A. Wienke, *Frailty models in survival analysis*, New York: Chapman & Hall/CRC, 2011. https://doi.org/10.1201/9781420073911
4. L. Duchateau, P. Janssen, *The frailty model*, New York: Springer, 2008. https://doi.org/10.1007/978-0-387-72835-3
5. P. Hougaard, Survival models for heterogeneous populations derived from stable distributions, *Biometrika*, **73** (1986), 387–396. https://doi.org/10.1093/biomet/73.2.387
6. P. Hougaard, Frailty models for survival data, *Lifetime Data Anal.*, **1** (1995), 255–273. https://doi.org/10.1007/BF00985760
7. A. Wienke, K. G. Arbeev, I. Locatelli, A. I. Yashin, A simulation study of different correlated frailty models and estimation strategies, *MPIDR Working Paper*, WP-2003-018. https://doi.org/10.4054/MPIDR-WP-2003-018

8. H. Loubna, H. Goual, F. M. Alghamdi, M. S. Mustafa, G. Tekle Mekiso, M. M. Ali, et al., The quasi-xgamma frailty model with survival analysis under heterogeneity problem, validation testing, and risk analysis for emergency care data, *Sci. Rep.*, **14** (2024), 8973. https://doi.org/10.1038/s41598-024-59137-w

9. M. Xie, J. Zhou, L. Liu, A double exponential gamma-frailty model for clustered survival data, *J. Nonparametr. Stat.*, **37** (2025), 772–795. https://doi.org/10.1080/10485252.2024.2304115

10. M. Rahmouni, A logarithmic gamma frailty model for first-failure times with heavy-tailed risk, *AIMS Mathematics*, **11** (2026), 8945–8965. https://doi.org/10.3934/math.2026369

11. G. Kiprotich, D. I. Gallardo, P. L. Ramos, T. Augustin, A shared frailty regression model for clustered survival data, *Stat. Methods Med. Res.*, **34** (2025), 1385–1412. https://doi.org/10.1177/09622802251338984

12. G. Kiprotich, D. I. Gallardo, P. L. Ramos, T. Augustin, On a new class of frailty regression models for clustered survival data, *J. Stat. Comput. Sim.*, **96** (2026), 1273–1302. https://doi.org/10.1080/00949655.2025.2584734

13. M. Ishag, I. Elbatal, A. Wanjoya, A. Adem, E. Almetwally, A. Afify, A new parametric Yang-Prentice regression model with applications to real-life survival medical data with crossing survival curves, *IEEE Access*, **13** (2025), 155462–155473. https://doi.org/10.1109/ACCESS.2025.3601730

14. E. Elsherpieny, A. Abdel-Hakim, Statistical analysis of alpha-power exponential distribution using unified hybrid censored data and its applications, *Computational Journal of Mathematical and Statistical Sciences*, **4** (2025), 283–315. https://doi.org/10.21608/cjmss.2025.346134.1094

15. R. Gupta, D. Kundu, Exponentiated exponential family: an alternative to gamma and Weibull distributions, *Biometrical J.*, **43** (2001), 117–130. https://doi.org/10.1002/1521-4036(200102)43:1¡117::AID-BIMJ117¿3.0.CO;2-R

16. S. Self, K. Liang, Asymptotic properties of maximum likelihood estimators and likelihood ratio tests under nonstandard conditions, *J. Am. Stat. Assoc.*, **82** (1987), 605–610. https://doi.org/10.2307/2289471

17. *Instituto Nacional de Salud, Sistema Nacional de Vigilancia en Salud Pública (SIVIGILA)*, Instituto Nacional de Salud of Colombia, 2024. Available at: `https://www.ins.gov.co/Direcciones/Vigilancia/Paginas/SIVIGILA.aspx`.

Appendix

A. Tables with more detailed numerical results of the simulation study

Tables 5–10 summarize in greater detail the finite-sample performance of the maximum likelihood estimation procedure considered in Section 4.

Table 5. Performance of the maximum likelihood estimator $\widehat{\beta}$ under the Weibull ($k = 0.7$) baseline model.

			Gamma frailty				EE frailty			
Var(V)	Cens.	n	Conv. (%)	Bias	SD	RMSE	Conv. (%)	Bias	SD	RMSE
0.281	0%	50	100.0	0.062	0.450	0.454	99.6	0.042	0.420	0.422
0.281	0%	100	100.0	0.009	0.278	0.278	100.0	0.013	0.271	0.271
0.281	0%	200	100.0	-0.002	0.197	0.197	100.0	0.005	0.195	0.195
0.281	0%	500	100.0	0.002	0.118	0.118	100.0	0.007	0.118	0.118
0.281	0%	1000	100.0	0.001	0.086	0.086	100.0	-0.005	0.084	0.084
0.281	30%	50	100.0	0.058	0.476	0.479	98.9	0.093	0.481	0.490
0.281	30%	100	100.0	0.036	0.319	0.321	98.6	0.048	0.324	0.327
0.281	30%	200	100.0	0.026	0.223	0.225	99.0	0.029	0.223	0.225
0.281	30%	500	100.0	-0.004	0.142	0.142	100.0	0.020	0.135	0.137
0.281	30%	1000	100.0	0.006	0.099	0.100	99.9	0.005	0.097	0.097
0.281	60%	50	100.0	0.084	0.625	0.631	94.3	0.115	0.597	0.608
0.281	60%	100	100.0	0.047	0.406	0.409	94.3	0.045	0.404	0.407
0.281	60%	200	100.0	0.036	0.268	0.270	93.5	0.050	0.264	0.268
0.281	60%	500	100.0	0.027	0.170	0.172	94.4	0.049	0.175	0.181
0.281	60%	1000	100.0	0.022	0.134	0.136	93.3	0.030	0.128	0.132
0.281	90%	50	78.4	-0.108	0.850	0.856	76.5	-0.095	0.822	0.827
0.281	90%	100	96.4	0.028	0.693	0.693	92.3	0.092	0.733	0.738
0.281	90%	200	100.0	0.034	0.528	0.528	97.4	0.052	0.528	0.531
0.281	90%	500	100.0	-0.006	0.315	0.315	99.0	0.025	0.322	0.323
0.281	90%	1000	100.0	0.006	0.210	0.210	98.1	0.023	0.223	0.224
0.556	0%	50	100.0	0.023	0.466	0.466	99.9	0.037	0.457	0.459
0.556	0%	100	100.0	0.023	0.334	0.335	100.0	0.027	0.329	0.330
0.556	0%	200	100.0	0.004	0.235	0.234	100.0	0.006	0.220	0.220
0.556	0%	500	100.0	0.003	0.147	0.146	100.0	-0.004	0.142	0.142
0.556	0%	1000	100.0	0.000	0.099	0.099	100.0	0.004	0.103	0.103
0.556	30%	50	100.0	0.026	0.500	0.500	99.0	0.041	0.502	0.503
0.556	30%	100	100.0	0.022	0.354	0.355	99.5	0.034	0.344	0.346
0.556	30%	200	100.0	0.013	0.243	0.243	99.4	0.023	0.229	0.230
0.556	30%	500	100.0	0.011	0.157	0.157	100.0	0.015	0.155	0.156
0.556	30%	1000	100.0	0.018	0.110	0.112	100.0	0.009	0.111	0.111
0.556	60%	50	100.0	0.084	0.588	0.594	96.4	0.061	0.599	0.601
0.556	60%	100	100.0	0.017	0.410	0.410	95.8	0.036	0.403	0.404
0.556	60%	200	100.0	0.026	0.278	0.279	96.1	0.023	0.281	0.282
0.556	60%	500	100.0	0.006	0.187	0.187	96.5	0.015	0.183	0.184
0.556	60%	1000	100.0	0.014	0.123	0.124	98.0	0.020	0.127	0.129
0.556	90%	50	78.0	-0.119	0.874	0.881	75.9	-0.135	0.905	0.914
0.556	90%	100	96.4	0.057	0.706	0.708	93.1	0.048	0.745	0.746
0.556	90%	200	99.9	0.032	0.487	0.487	97.8	0.085	0.566	0.572
0.556	90%	500	100.0	-0.023	0.307	0.308	98.7	0.024	0.332	0.332
0.556	90%	1000	100.0	-0.037	0.214	0.218	99.1	0.018	0.224	0.224

Table 6. Performance of the maximum likelihood estimator $\widehat{\beta}$ under the Weibull ($k = 1.5$) baseline model.

			Gamma frailty				EE frailty			
Var(V)	Cens.	n	Conv. (%)	Bias	SD	RMSE	Conv. (%)	Bias	SD	RMSE
0.281	0%	50	100.0	0.041	0.432	0.434	99.9	0.058	0.426	0.429
0.281	0%	100	100.0	0.024	0.295	0.296	100.0	0.022	0.280	0.281
0.281	0%	200	100.0	0.011	0.199	0.199	100.0	0.010	0.190	0.190
0.281	0%	500	100.0	-0.000	0.121	0.121	100.0	0.008	0.117	0.117
0.281	0%	1000	100.0	0.002	0.085	0.085	100.0	-0.004	0.082	0.082
0.281	30%	50	100.0	0.054	0.510	0.512	98.7	0.076	0.501	0.507
0.281	30%	100	100.0	0.043	0.332	0.334	99.3	0.057	0.330	0.334
0.281	30%	200	100.0	0.016	0.235	0.236	99.4	0.024	0.220	0.222
0.281	30%	500	100.0	-0.011	0.142	0.143	99.9	0.009	0.137	0.137
0.281	30%	1000	100.0	-0.001	0.102	0.102	100.0	0.001	0.098	0.098
0.281	60%	50	100.0	0.068	0.627	0.630	96.3	0.061	0.626	0.629
0.281	60%	100	100.0	0.075	0.423	0.429	97.7	0.096	0.399	0.410
0.281	60%	200	100.0	0.036	0.280	0.283	97.2	0.043	0.282	0.285
0.281	60%	500	100.0	0.011	0.178	0.179	97.1	0.025	0.179	0.181
0.281	60%	1000	100.0	0.014	0.130	0.131	97.5	0.001	0.122	0.122
0.281	90%	50	80.4	-0.068	0.987	0.989	73.0	-0.020	0.992	0.992
0.281	90%	100	97.0	0.081	0.806	0.810	85.0	0.102	0.823	0.829
0.281	90%	200	100.0	0.088	0.561	0.567	89.7	0.078	0.576	0.581
0.281	90%	500	100.0	0.034	0.335	0.336	92.8	0.064	0.331	0.337
0.281	90%	1000	100.0	0.046	0.230	0.234	94.1	0.036	0.232	0.234
0.556	0%	50	100.0	0.036	0.492	0.493	99.9	0.042	0.478	0.480
0.556	0%	100	100.0	0.009	0.340	0.340	100.0	0.012	0.321	0.321
0.556	0%	200	100.0	0.012	0.239	0.239	100.0	-0.006	0.218	0.217
0.556	0%	500	100.0	0.000	0.139	0.138	100.0	0.004	0.142	0.142
0.556	0%	1000	100.0	-0.003	0.101	0.101	100.0	-0.004	0.097	0.097
0.556	30%	50	100.0	0.029	0.522	0.523	99.0	0.030	0.510	0.511
0.556	30%	100	100.0	0.014	0.350	0.350	99.6	0.018	0.346	0.346
0.556	30%	200	100.0	0.001	0.248	0.248	99.9	0.025	0.246	0.247
0.556	30%	500	100.0	0.018	0.159	0.160	100.0	0.017	0.152	0.153
0.556	30%	1000	100.0	0.005	0.109	0.109	100.0	0.011	0.109	0.109
0.556	60%	50	100.0	0.112	0.641	0.651	97.3	0.071	0.633	0.637
0.556	60%	100	100.0	0.018	0.432	0.433	96.9	0.038	0.441	0.442
0.556	60%	200	100.0	0.018	0.295	0.296	97.1	0.021	0.288	0.288
0.556	60%	500	100.0	0.013	0.193	0.193	99.1	0.014	0.190	0.191
0.556	60%	1000	100.0	0.018	0.131	0.132	99.5	0.007	0.135	0.135
0.556	90%	50	80.3	-0.098	1.025	1.029	73.0	-0.069	1.017	1.019
0.556	90%	100	97.0	0.035	0.792	0.792	86.5	0.045	0.818	0.818
0.556	90%	200	100.0	0.084	0.592	0.598	92.4	0.074	0.601	0.605
0.556	90%	500	100.0	0.002	0.337	0.337	95.3	0.032	0.325	0.327
0.556	90%	1000	100.0	0.024	0.235	0.236	95.9	0.022	0.235	0.236

Table 7. Performance of the maximum likelihood estimator $\widehat{\beta}$ under the log-normal ($\sigma = 0.6$) baseline model.

			Gamma frailty				EE frailty			
Var(V)	Cens.	n	Conv. (%)	Bias	SD	RMSE	Conv. (%)	Bias	SD	RMSE
0.281	0%	50	100.0	-0.009	0.246	0.246	100.0	-0.001	0.233	0.233
0.281	0%	100	100.0	0.002	0.169	0.169	100.0	0.000	0.164	0.164
0.281	0%	200	100.0	-0.002	0.118	0.118	100.0	-0.007	0.112	0.112
0.281	0%	500	100.0	0.002	0.072	0.072	100.0	0.000	0.073	0.073
0.281	0%	1000	100.0	0.003	0.052	0.052	100.0	-0.002	0.051	0.051
0.281	30%	50	100.0	-0.003	0.276	0.276	100.0	0.011	0.264	0.264
0.281	30%	100	100.0	-0.004	0.187	0.187	100.0	-0.009	0.182	0.182
0.281	30%	200	100.0	-0.004	0.129	0.129	100.0	-0.000	0.128	0.128
0.281	30%	500	100.0	-0.000	0.082	0.082	100.0	-0.002	0.080	0.080
0.281	30%	1000	100.0	-0.000	0.056	0.056	100.0	0.001	0.055	0.055
0.281	60%	50	99.7	0.026	0.317	0.317	100.0	-0.007	0.331	0.331
0.281	60%	100	100.0	0.010	0.222	0.223	99.9	0.004	0.220	0.220
0.281	60%	200	100.0	0.001	0.154	0.154	100.0	0.000	0.154	0.154
0.281	60%	500	100.0	0.005	0.093	0.093	100.0	0.000	0.094	0.094
0.281	60%	1000	100.0	-0.001	0.068	0.068	100.0	0.001	0.066	0.066
0.281	90%	50	65.5	0.664	1.534	1.670	61.7	0.544	1.389	1.491
0.281	90%	100	90.6	0.146	0.812	0.825	86.8	0.110	0.768	0.775
0.281	90%	200	99.0	0.018	0.351	0.351	97.5	0.041	0.345	0.347
0.281	90%	500	100.0	0.018	0.166	0.167	97.4	0.011	0.166	0.166
0.281	90%	1000	100.0	0.008	0.112	0.112	97.3	0.005	0.120	0.120
0.556	0%	50	100.0	0.010	0.309	0.309	100.0	-0.011	0.304	0.304
0.556	0%	100	100.0	0.003	0.212	0.212	100.0	0.002	0.206	0.206
0.556	0%	200	100.0	-0.004	0.142	0.142	100.0	-0.000	0.145	0.145
0.556	0%	500	100.0	0.004	0.090	0.090	100.0	-0.000	0.086	0.086
0.556	0%	1000	100.0	-0.001	0.066	0.066	100.0	-0.001	0.062	0.062
0.556	30%	50	100.0	0.007	0.330	0.330	100.0	-0.007	0.326	0.326
0.556	30%	100	100.0	0.002	0.228	0.228	100.0	0.011	0.221	0.221
0.556	30%	200	100.0	0.008	0.151	0.152	100.0	-0.001	0.152	0.152
0.556	30%	500	100.0	0.001	0.098	0.098	100.0	-0.001	0.096	0.096
0.556	30%	1000	100.0	-0.001	0.068	0.068	100.0	-0.002	0.067	0.067
0.556	60%	50	99.8	0.009	0.347	0.347	99.7	0.008	0.370	0.370
0.556	60%	100	100.0	0.002	0.250	0.250	99.8	0.006	0.250	0.250
0.556	60%	200	100.0	0.000	0.178	0.178	100.0	-0.006	0.179	0.179
0.556	60%	500	100.0	-0.001	0.112	0.112	100.0	0.007	0.107	0.107
0.556	60%	1000	100.0	0.001	0.078	0.078	100.0	0.003	0.077	0.077
0.556	90%	50	68.8	0.335	1.306	1.347	62.4	0.335	1.322	1.363
0.556	90%	100	89.4	0.084	0.725	0.729	87.8	0.065	0.683	0.685
0.556	90%	200	98.5	0.019	0.292	0.293	98.0	0.033	0.308	0.310
0.556	90%	500	100.0	-0.004	0.179	0.179	97.5	0.013	0.185	0.185
0.556	90%	1000	100.0	0.002	0.125	0.125	97.3	0.003	0.126	0.126

Table 8. Performance of the estimator of Var(V) under the Weibull PH ($k = 0.7$) model.

			Gamma frailty			EE frailty		
Var(V)	Cens.	n	Bias	SD	RMSE	Bias	SD	RMSE
0.281	0%	50	0.032	0.370	0.371	0.057	0.299	0.304
0.281	0%	100	−0.005	0.253	0.253	0.015	0.200	0.201
0.281	0%	200	−0.016	0.175	0.176	−0.007	0.134	0.134
0.281	0%	500	−0.008	0.105	0.105	−0.009	0.092	0.093
0.281	0%	1000	−0.002	0.069	0.069	−0.007	0.071	0.071
0.281	30%	50	0.126	0.416	0.435	0.146	0.349	0.379
0.281	30%	100	0.054	0.341	0.345	0.111	0.302	0.321
0.281	30%	200	0.043	0.286	0.289	0.071	0.245	0.255
0.281	30%	500	0.017	0.215	0.216	0.029	0.175	0.177
0.281	30%	1000	0.011	0.147	0.148	0.008	0.127	0.127
0.281	60%	50	0.215	0.451	0.499	0.258	0.388	0.466
0.281	60%	100	0.171	0.419	0.452	0.263	0.363	0.448
0.281	60%	200	0.149	0.394	0.421	0.213	0.340	0.401
0.281	60%	500	0.124	0.354	0.375	0.183	0.317	0.366
0.281	60%	1000	0.155	0.335	0.369	0.177	0.302	0.349
0.281	90%	50	−0.035	0.389	0.390	0.457	0.277	0.534
0.281	90%	100	−0.125	0.324	0.347	0.455	0.267	0.527
0.281	90%	200	−0.189	0.254	0.316	0.448	0.263	0.520
0.281	90%	500	−0.256	0.121	0.284	0.511	0.183	0.543
0.281	90%	1000	−0.270	0.064	0.277	0.542	0.114	0.554
0.556	0%	50	−0.004	0.420	0.420	−0.012	0.365	0.365
0.556	0%	100	−0.004	0.292	0.292	−0.001	0.292	0.292
0.556	0%	200	−0.001	0.221	0.221	−0.001	0.206	0.206
0.556	0%	500	−0.001	0.142	0.142	−0.005	0.127	0.128
0.556	0%	1000	−0.003	0.101	0.101	−0.005	0.086	0.086
0.556	30%	50	−0.005	0.429	0.428	0.023	0.377	0.378
0.556	30%	100	−0.016	0.363	0.363	0.013	0.329	0.329
0.556	30%	200	−0.002	0.309	0.309	0.030	0.276	0.277
0.556	30%	500	0.033	0.218	0.220	0.034	0.212	0.214
0.556	30%	1000	0.055	0.173	0.181	0.038	0.177	0.181
0.556	60%	50	−0.029	0.452	0.453	0.065	0.387	0.392
0.556	60%	100	−0.011	0.415	0.415	0.058	0.354	0.359
0.556	60%	200	−0.003	0.385	0.385	0.048	0.337	0.341
0.556	60%	500	0.022	0.339	0.339	0.084	0.299	0.310
0.556	60%	1000	0.078	0.289	0.299	0.124	0.257	0.286
0.556	90%	50	−0.285	0.400	0.490	0.180	0.283	0.335
0.556	90%	100	−0.375	0.343	0.508	0.185	0.262	0.321
0.556	90%	200	−0.465	0.252	0.529	0.197	0.240	0.311
0.556	90%	500	−0.531	0.122	0.545	0.243	0.171	0.297
0.556	90%	1000	−0.548	0.037	0.549	0.280	0.066	0.288

Table 9. Performance of the estimator of Var(V) under the Weibull PH ($k = 1.5$) model.

			Gamma frailty			EE frailty		
Var(V)	Cens.	n	Bias	SD	RMSE	Bias	SD	RMSE
0.281	0%	50	0.007	0.341	0.341	0.047	0.286	0.290
0.281	0%	100	0.009	0.255	0.255	0.016	0.205	0.205
0.281	0%	200	−0.011	0.171	0.171	−0.008	0.136	0.136
0.281	0%	500	−0.009	0.098	0.098	−0.008	0.093	0.093
0.281	0%	1000	−0.002	0.066	0.066	−0.011	0.071	0.071
0.281	30%	50	0.059	0.404	0.408	0.118	0.336	0.356
0.281	30%	100	0.033	0.313	0.315	0.052	0.254	0.259
0.281	30%	200	0.011	0.248	0.248	0.029	0.197	0.199
0.281	30%	500	−0.002	0.160	0.160	0.009	0.140	0.141
0.281	30%	1000	−0.002	0.111	0.111	−0.002	0.096	0.096
0.281	60%	50	0.125	0.440	0.457	0.178	0.379	0.418
0.281	60%	100	0.118	0.390	0.407	0.156	0.337	0.371
0.281	60%	200	0.079	0.343	0.352	0.130	0.299	0.326
0.281	60%	500	0.044	0.279	0.282	0.064	0.243	0.251
0.281	60%	1000	0.027	0.226	0.227	0.034	0.193	0.196
0.281	90%	50	0.182	0.444	0.480	0.391	0.341	0.518
0.281	90%	100	0.206	0.426	0.473	0.393	0.322	0.508
0.281	90%	200	0.214	0.412	0.464	0.373	0.321	0.492
0.281	90%	500	0.231	0.400	0.462	0.368	0.314	0.483
0.281	90%	1000	0.276	0.382	0.471	0.410	0.285	0.499
0.556	0%	50	−0.028	0.408	0.409	0.007	0.370	0.370
0.556	0%	100	−0.005	0.307	0.307	−0.010	0.273	0.273
0.556	0%	200	−0.010	0.221	0.221	−0.001	0.199	0.199
0.556	0%	500	−0.003	0.134	0.134	−0.001	0.126	0.126
0.556	0%	1000	−0.008	0.101	0.101	−0.004	0.085	0.086
0.556	30%	50	−0.037	0.425	0.427	−0.001	0.375	0.375
0.556	30%	100	−0.021	0.356	0.356	−0.015	0.307	0.307
0.556	30%	200	−0.010	0.273	0.273	0.019	0.251	0.251
0.556	30%	500	0.027	0.188	0.190	0.022	0.173	0.175
0.556	30%	1000	0.032	0.138	0.141	0.023	0.136	0.138
0.556	60%	50	−0.024	0.450	0.450	0.015	0.392	0.392
0.556	60%	100	−0.041	0.411	0.413	0.032	0.352	0.353
0.556	60%	200	−0.001	0.353	0.352	0.023	0.317	0.317
0.556	60%	500	0.027	0.288	0.289	0.042	0.262	0.266
0.556	60%	1000	0.076	0.221	0.234	0.066	0.228	0.237
0.556	90%	50	−0.091	0.439	0.448	0.099	0.348	0.362
0.556	90%	100	−0.050	0.422	0.424	0.117	0.322	0.342
0.556	90%	200	−0.024	0.405	0.405	0.126	0.306	0.331
0.556	90%	500	0.017	0.382	0.382	0.170	0.266	0.315
0.556	90%	1000	0.071	0.352	0.359	0.213	0.214	0.302

Table 10. Performance of the estimator of Var(V) under the log-normal AFT model.

			Gamma frailty			EE frailty		
Var(V)	Cens.	n	Bias	SD	RMSE	Bias	SD	RMSE
0.281	0%	50	−0.045	0.209	0.214	0.009	0.150	0.150
0.281	0%	100	−0.045	0.176	0.182	−0.001	0.132	0.132
0.281	0%	200	−0.040	0.146	0.151	−0.008	0.114	0.114
0.281	0%	500	−0.018	0.097	0.098	−0.019	0.088	0.090
0.281	0%	1000	−0.010	0.069	0.070	−0.017	0.075	0.077
0.281	30%	50	−0.006	0.252	0.251	0.039	0.192	0.196
0.281	30%	100	−0.016	0.219	0.219	0.025	0.168	0.170
0.281	30%	200	−0.019	0.187	0.188	0.018	0.139	0.140
0.281	30%	500	−0.023	0.139	0.141	−0.005	0.112	0.112
0.281	30%	1000	−0.019	0.109	0.111	−0.013	0.092	0.092
0.281	60%	50	0.042	0.312	0.315	0.105	0.253	0.274
0.281	60%	100	0.048	0.287	0.290	0.079	0.227	0.240
0.281	60%	200	0.013	0.252	0.252	0.061	0.196	0.206
0.281	60%	500	−0.001	0.193	0.192	0.016	0.148	0.149
0.281	60%	1000	−0.023	0.139	0.141	0.003	0.123	0.123
0.281	90%	50	0.084	0.355	0.365	0.170	0.304	0.348
0.281	90%	100	0.129	0.354	0.376	0.215	0.304	0.373
0.281	90%	200	0.185	0.353	0.399	0.225	0.310	0.383
0.281	90%	500	0.172	0.347	0.387	0.199	0.304	0.363
0.281	90%	1000	0.134	0.331	0.357	0.175	0.287	0.336
0.556	0%	50	−0.104	0.261	0.281	−0.072	0.228	0.239
0.556	0%	100	−0.077	0.206	0.219	−0.061	0.181	0.191
0.556	0%	200	−0.054	0.139	0.149	−0.045	0.134	0.141
0.556	0%	500	−0.028	0.076	0.081	−0.027	0.077	0.082
0.556	0%	1000	−0.029	0.052	0.059	−0.019	0.050	0.053
0.556	30%	50	−0.058	0.349	0.353	−0.051	0.291	0.296
0.556	30%	100	−0.039	0.293	0.296	−0.029	0.253	0.254
0.556	30%	200	−0.018	0.227	0.228	−0.027	0.208	0.209
0.556	30%	500	−0.012	0.145	0.146	0.000	0.139	0.139
0.556	30%	1000	0.009	0.100	0.100	0.003	0.099	0.099
0.556	60%	50	−0.016	0.392	0.392	0.018	0.339	0.339
0.556	60%	100	−0.032	0.360	0.362	−0.015	0.317	0.317
0.556	60%	200	−0.020	0.318	0.319	0.003	0.281	0.281
0.556	60%	500	0.004	0.235	0.235	0.016	0.221	0.221
0.556	60%	1000	0.030	0.180	0.182	0.016	0.180	0.181
0.556	90%	50	−0.076	0.384	0.392	0.002	0.328	0.328
0.556	90%	100	−0.003	0.376	0.376	0.043	0.330	0.333
0.556	90%	200	0.040	0.367	0.369	0.067	0.328	0.334
0.556	90%	500	0.058	0.340	0.344	0.115	0.294	0.316
0.556	90%	1000	0.102	0.300	0.316	0.125	0.273	0.301

B. Score functions and observed information matrix

The analytical derivations in this appendix apply exclusively to the multiplicative EE frailty model under the proportional hazards specification $h(t \mid \mathbf{X}, V) = Vh_0(t;\Theta)\exp(\mathbf{X}^\top\boldsymbol{\beta})$. They do not apply to the log-normal AFT frailty formulation defined in (2.9), for which the frailty enters the location of log-survival time through $-\log(V)$. For the AFT model, the marginal likelihood, score vector, and observed Hessian are evaluated numerically after integration over the frailty distribution. For the proportional hazards model, let $\boldsymbol{\Omega} = (\alpha, \Theta^\top, \boldsymbol{\beta}^\top)^\top$, where α denotes the frailty parameter, $\Theta = (\theta_1, \ldots, \theta_r)^\top$ contains the baseline-hazard parameters, and $\boldsymbol{\beta} = (\beta_1, \ldots, \beta_p)^\top$ contains the regression coefficients. The score vector is defined as

$$U(\boldsymbol{\Omega}) = \frac{\partial \ell(\boldsymbol{\Omega})}{\partial \boldsymbol{\Omega}} = (U(\alpha), U(\Theta), U(\boldsymbol{\beta}))^\top . \tag{B.1}$$

B.1. Score function for the frailty parameter

The score component associated with the frailty parameter α is

$$\begin{aligned}
U(\alpha) &= -\frac{\psi'(\alpha+1)}{\psi(\alpha+1)-\psi(1)}\sum_{i=1}^{n}\delta_i + n\left(\psi(\alpha)+\frac{1}{\alpha}\right) - \sum_{i=1}^{n}\psi\left(\alpha+\frac{H_0(t_i,\Theta)e^{\mathbf{X}_i^\top\boldsymbol{\beta}}}{\psi(\alpha+1)-\psi(1)}+1\right) \\
&+ \sum_{i=1}^{n}\frac{\psi'(\alpha+1)H_0(t_i,\Theta)e^{\mathbf{X}_i^\top\boldsymbol{\beta}}}{(\psi(\alpha+1)-\psi(1))^2}\left(\psi\left(\alpha+\frac{H_0(t_i,\Theta)e^{\mathbf{X}_i^\top\boldsymbol{\beta}}}{\psi(\alpha+1)-\psi(1)}+1\right)-\psi\left(\frac{H_0(t_i,\Theta)e^{\mathbf{X}_i^\top\boldsymbol{\beta}}}{\psi(\alpha+1)-\psi(1)}+1\right)\right) \\
&+ \sum_{i=1}^{n}\delta_i\frac{\psi'\left(\alpha+\frac{H_0(t_i,\Theta)e^{\mathbf{X}_i^\top\boldsymbol{\beta}}}{\psi(\alpha+1)-\psi(1)}+1\right)}{\psi\left(\alpha+\frac{H_0(t_i,\Theta)e^{\mathbf{X}_i^\top\boldsymbol{\beta}}}{\psi(\alpha+1)-\psi(1)}+1\right)-\psi\left(\frac{H_0(t_i,\Theta)e^{\mathbf{X}_i^\top\boldsymbol{\beta}}}{\psi(\alpha+1)-\psi(1)}+1\right)} \\
&- \sum_{i=1}^{n}\delta_i\frac{\psi'(\alpha+1)H_0(t_i,\Theta)e^{\mathbf{X}_i^\top\boldsymbol{\beta}}}{(\psi(\alpha+1)-\psi(1))^2}\frac{\psi'\left(\alpha+\frac{H_0(t_i,\Theta)e^{\mathbf{X}_i^\top\boldsymbol{\beta}}}{\psi(\alpha+1)-\psi(1)}+1\right)-\psi'\left(\frac{H_0(t_i,\Theta)e^{\mathbf{X}_i^\top\boldsymbol{\beta}}}{\psi(\alpha+1)-\psi(1)}+1\right)}{\psi\left(\alpha+\frac{H_0(t_i,\Theta)e^{\mathbf{X}_i^\top\boldsymbol{\beta}}}{\psi(\alpha+1)-\psi(1)}+1\right)-\psi\left(\frac{H_0(t_i,\Theta)e^{\mathbf{X}_i^\top\boldsymbol{\beta}}}{\psi(\alpha+1)-\psi(1)}+1\right)}.
\end{aligned}$$

B.2. Score functions for baseline hazard parameters

For $k = 1, \ldots, r$, the score components associated with θ_k are

$$\begin{aligned}
U(\theta_k) &= \sum_{i=1}^{n}\delta_i\frac{\frac{\partial}{\partial\theta_k}H_0(t_i,\Theta)e^{\mathbf{X}_i^\top\boldsymbol{\beta}}}{\psi(\alpha+1)-\psi(1)}\frac{\psi'\left(\alpha+\frac{H_0(t_i,\Theta)e^{\mathbf{X}_i^\top\boldsymbol{\beta}}}{\psi(\alpha+1)-\psi(1)}+1\right)-\psi'\left(\frac{H_0(t_i,\Theta)e^{\mathbf{X}_i^\top\boldsymbol{\beta}}}{\psi(\alpha+1)-\psi(1)}+1\right)}{\psi\left(\alpha+\frac{H_0(t_i,\Theta)e^{\mathbf{X}_i^\top\boldsymbol{\beta}}}{\psi(\alpha+1)-\psi(1)}+1\right)-\psi\left(\frac{H_0(t_i,\Theta)e^{\mathbf{X}_i^\top\boldsymbol{\beta}}}{\psi(\alpha+1)-\psi(1)}+1\right)} \\
&+ \sum_{i=1}^{n}\delta_i\frac{\frac{\partial}{\partial\theta_k}h_0(t_i,\Theta)}{h_0(t_i,\Theta)} \\
&- \sum_{i=1}^{n}\frac{\frac{\partial}{\partial\theta_k}H_0(t_i,\Theta)e^{\mathbf{X}_i^\top\boldsymbol{\beta}}}{\psi(\alpha+1)-\psi(1)}\left(\psi\left(\alpha+\frac{H_0(t_i,\Theta)e^{\mathbf{X}_i^\top\boldsymbol{\beta}}}{\psi(\alpha+1)-\psi(1)}+1\right)-\psi\left(\frac{H_0(t_i,\Theta)e^{\mathbf{X}_i^\top\boldsymbol{\beta}}}{\psi(\alpha+1)-\psi(1)}+1\right)\right).
\end{aligned}$$

B.3. Score functions for regression parameters

For $j = 1, \ldots, p$, the score components corresponding to the regression coefficients are

$$\begin{aligned} U(\beta_j) &= -\sum_{i=1}^{n} X_{ij} \frac{H_0(t_i,\Theta)e^{\mathbf{X}_i^\top\beta}}{\psi(\alpha+1)-\psi(1)} \left(\psi\left(\alpha+\frac{H_0(t_i,\Theta)e^{\mathbf{X}_i^\top\beta}}{\psi(\alpha+1)-\psi(1)}+1\right)-\psi\left(\frac{H_0(t_i,\Theta)e^{\mathbf{X}_i^\top\beta}}{\psi(\alpha+1)-\psi(1)}+1\right)\right) \\ &+ \sum_{i=1}^{n}\delta_i X_{ij} + \sum_{i=1}^{n}\delta_i X_{ij}\frac{H_0(t_i,\Theta)e^{\mathbf{X}_i^\top\beta}}{\psi(\alpha+1)-\psi(1)} \frac{\psi'\left(\alpha+\frac{H_0(t_i,\Theta)e^{\mathbf{X}_i^\top\beta}}{\psi(\alpha+1)-\psi(1)}+1\right)-\psi'\left(\frac{H_0(t_i,\Theta)e^{\mathbf{X}_i^\top\beta}}{\psi(\alpha+1)-\psi(1)}+1\right)}{\psi\left(\alpha+\frac{H_0(t_i,\Theta)e^{\mathbf{X}_i^\top\beta}}{\psi(\alpha+1)-\psi(1)}+1\right)-\psi\left(\frac{H_0(t_i,\Theta)e^{\mathbf{X}_i^\top\beta}}{\psi(\alpha+1)-\psi(1)}+1\right)}. \end{aligned}$$

B.4. Auxiliary quantities

To simplify the presentation of the observed information matrix, define $\omega_i = \frac{\psi'(\alpha+\xi_i+1)-\psi'(\xi_i+1)}{\psi(\alpha+\xi_i+1)-\psi(\xi_i+1)}$, $\omega_i' = \frac{\psi''(\alpha+\xi_i+1)-\psi''(\xi_i+1)}{\psi(\alpha+\xi_i+1)-\psi(\xi_i+1)}$, and $\tau_{ik} = \frac{\psi'(\alpha+1)H_0(t_i,\Theta)e^{\mathbf{x}_i^\top\beta}}{\left[\psi(\alpha+1)-\psi(1)\right]^k}$.

B.5. Observed information matrix

The observed information matrix is defined as $J(\boldsymbol{\Omega}) = -\frac{\partial^2\ell(\boldsymbol{\Omega})}{\partial\boldsymbol{\Omega}\partial\boldsymbol{\Omega}^\top}$. Its block representation is

$$J(\boldsymbol{\Omega}) = \begin{pmatrix} J_{\alpha\alpha} & J_{\alpha\Theta} & J_{\alpha\beta} \\ J_{\Theta\alpha} & J_{\Theta\Theta} & J_{\Theta\beta} \\ J_{\beta\alpha} & J_{\beta\Theta} & J_{\beta\beta} \end{pmatrix}. \tag{B.2}$$

B.5.1. Element $j_{\alpha\alpha}$

$$\begin{aligned} j_{\alpha\alpha} &= \left(\frac{\psi''(\alpha+1)}{\psi(\alpha+1)-\psi(1)} - \left(\frac{\psi'(\alpha+1)}{\psi(\alpha+1)-\psi(1)}\right)^2\right)\sum_{i=1}^{n}\delta_i + n\left(\frac{1}{\alpha^2}-\psi'(\alpha)\right) \\ &+ \sum_{i=1}^{n}\left((1-\tau_{i2})^2\psi'\left(\alpha+\frac{H_0(t_i,\Theta)e^{\mathbf{X}_i^\top\beta}}{\psi(\alpha+1)-\psi(1)}+1\right)-\tau_{i2}^2\psi'\left(\frac{H_0(t_i,\Theta)e^{\mathbf{X}_i^\top\beta}}{\psi(\alpha+1)-\psi(1)}+1\right)\right) \\ &- \sum_{i=1}^{n}\tau_{i2}\left(\frac{\psi''(\alpha+1)}{\psi'(\alpha+1)}-\frac{2\psi'(\alpha+1)}{\psi(\alpha+1)-\psi(1)}\right)\left(\psi\left(\alpha+\frac{H_0(t_i,\Theta)e^{\mathbf{X}_i^\top\beta}}{\psi(\alpha+1)-\psi(1)}+1\right)-\psi\left(\frac{H_0(t_i,\Theta)e^{\mathbf{X}_i^\top\beta}}{\psi(\alpha+1)-\psi(1)}+1\right)-\delta_i\omega_i\right) \\ &- \sum_{i=1}^{n}\delta_i\frac{(1-2\tau_{i2})\psi''\left(\alpha+\frac{H_0(t_i,\Theta)e^{\mathbf{X}_i^\top\beta}}{\psi(\alpha+1)-\psi(1)}+1\right)}{\psi\left(\alpha+\frac{H_0(t_i,\Theta)e^{\mathbf{X}_i^\top\beta}}{\psi(\alpha+1)-\psi(1)}+1\right)-\psi\left(\frac{H_0(t_i,\Theta)e^{\mathbf{X}_i^\top\beta}}{\psi(\alpha+1)-\psi(1)}+1\right)} - \sum_{i=1}^{n}\delta_i\tau_{i2}^2\omega_i' \\ &+ \sum_{i=1}^{n}\delta_i\frac{\psi'\left(\frac{H_0(t_i,\Theta)e^{\mathbf{X}_i^\top\beta}}{\psi(\alpha+1)-\psi(1)}+1\right)\left((1-\tau_{i2})\psi'\left(\alpha+\frac{H_0(t_i,\Theta)e^{\mathbf{X}_i^\top\beta}}{\psi(\alpha+1)-\psi(1)}+1\right)+\tau_{i2}\psi'\left(\frac{H_0(t_i,\Theta)e^{\mathbf{X}_i^\top\beta}}{\psi(\alpha+1)-\psi(1)}+1\right)\right)}{\left(\psi\left(\alpha+\frac{H_0(t_i,\Theta)e^{\mathbf{X}_i^\top\beta}}{\psi(\alpha+1)-\psi(1)}+1\right)-\psi\left(\frac{H_0(t_i,\Theta)e^{\mathbf{X}_i^\top\beta}}{\psi(\alpha+1)-\psi(1)}+1\right)\right)^2}. \end{aligned} \tag{B.3}$$

B.5.2. Elements $j_{\theta_k\alpha}$

For $k, k' = 1, 2, \ldots r$

$$
\begin{aligned}
j_{\theta_k\alpha} &= -\sum_{i=1}^{n} \tau_{i3} e^{\mathbf{X}_i^\top \beta} \frac{\partial}{\partial \theta_k} H_0(t_i, \Theta) \left(\psi\left(\alpha + \frac{H_0(t_i, \Theta) e^{\mathbf{X}_i^\top \beta}}{\psi(\alpha+1) - \psi(1)} + 1 \right) - \psi\left(\frac{H_0(t_i, \Theta) e^{\mathbf{X}_i^\top \beta}}{\psi(\alpha+1) - \psi(1)} + 1 \right) \right) \\
&- \sum_{i=1}^{n} \frac{\psi'(\alpha+1) e^{\mathbf{X}_i^\top \beta} \frac{\partial}{\partial \theta_k} H_0(t_i, \Theta)}{(\psi(\alpha+1) - \psi(1))^2} \left(\psi\left(\alpha + \frac{H_0(t_i, \Theta) e^{\mathbf{X}_i^\top \beta}}{\psi(\alpha+1) - \psi(1)} + 1 \right) - \psi\left(\frac{H_0(t_i, \Theta) e^{\mathbf{X}_i^\top \beta}}{\psi(\alpha+1) - \psi(1)} + 1 \right) \right) \\
&+ \sum_{i=1}^{n} \frac{e^{\mathbf{X}_i^\top \beta} \frac{\partial}{\partial \theta_k} H_0(t_i, \Theta)}{\psi(\alpha+1) - \psi(1)} \psi'\left(\alpha + \frac{H_0(t_i, \Theta) e^{\mathbf{X}_i^\top \beta}}{\psi(\alpha+1) - \psi(1)} + 1 \right) \\
&- \sum_{i=1}^{n} \frac{\delta_i e^{\mathbf{X}_i^\top \beta} \frac{\partial}{\partial \theta_k} H_0(t_i, \Theta) \psi''\left(\alpha + \frac{H_0(t_i, \Theta) e^{\mathbf{X}_i^\top \beta}}{\psi(\alpha+1) - \psi(1)} + 1 \right)}{(\psi(\alpha+1) - \psi(1)) \left(\psi\left(\alpha + \frac{H_0(t_i, \Theta) e^{\mathbf{X}_i^\top \beta}}{\psi(\alpha+1) - \psi(1)} + 1 \right) - \psi\left(\frac{H_0(t_i, \Theta) e^{\mathbf{X}_i^\top \beta}}{\psi(\alpha+1) - \psi(1)} + 1 \right) \right)} \\
&+ \sum_{i=1}^{n} \frac{\delta_i e^{\mathbf{X}_i^\top \beta} \omega_i' \frac{\partial}{\partial \theta_k} H_0(t_i, \Theta) \psi'\left(\alpha + \frac{H_0(t_i, \Theta) e^{\mathbf{X}_i^\top \beta}}{\psi(\alpha+1) - \psi(1)} + 1 \right)}{(\psi(\alpha+1) - \psi(1)) \left(\psi\left(\alpha + \frac{H_0(t_i, \Theta) e^{\mathbf{X}_i^\top \beta}}{\psi(\alpha+1) - \psi(1)} + 1 \right) - \psi\left(\frac{H_0(t_i, \Theta) e^{\mathbf{X}_i^\top \beta}}{\psi(\alpha+1) - \psi(1)} + 1 \right) \right)} \\
&+ \sum_{i=1}^{n} \frac{\delta_i e^{\mathbf{X}_i^\top \beta} \frac{\partial}{\partial \theta_k} H_0(t_i, \Theta)}{(\psi(\alpha+1) - \psi(1))^2} \left[\tau_{i1} (\omega_i' - \omega_i^2) + \psi'(\alpha+1) \omega_i \right] \quad k = 1, 2, \ldots r. \qquad \text{(B.4)}
\end{aligned}
$$

B.5.3. Elements $j_{\beta_j\alpha}$

$$
\begin{aligned}
j_{\beta_j\alpha} &= -\sum_{i=1}^{n} X_{ij} \tau_{i2} \left(\psi\left(\alpha + \frac{H_0(t_i, \Theta) e^{\mathbf{X}_i^\top \beta}}{\psi(\alpha+1) - \psi(1)} + 1 \right) - \psi\left(\frac{H_0(t_i, \Theta) e^{\mathbf{X}_i^\top \beta}}{\psi(\alpha+1) - \psi(1)} + 1 \right) \right) \\
&+ \sum_{i=1}^{n} X_{ij} \frac{\tau_{i1}}{\psi'(\alpha+1)} \psi'\left(\alpha + \frac{H_0(t_i, \Theta) e^{\mathbf{X}_i^\top \beta}}{\psi(\alpha+1) - \psi(1)} + 1 \right) \\
&- \sum_{i=1}^{n} X_{ij} \frac{\tau_{i1} \tau_{i2}}{\psi'(\alpha+1)} \left(\psi'\left(\alpha + \frac{H_0(t_i, \Theta) e^{\mathbf{X}_i^\top \beta}}{\psi(\alpha+1) - \psi(1)} + 1 \right) - \psi'\left(\frac{H_0(t_i, \Theta) e^{\mathbf{X}_i^\top \beta}}{\psi(\alpha+1) - \psi(1)} + 1 \right) \right) \\
&+ \sum_{i=1}^{n} \delta_i X_{ij} \frac{\tau_{i1}}{\psi'(\alpha+1)} \frac{\psi''\left(\alpha + \frac{H_0(t_i, \Theta) e^{\mathbf{X}_i^\top \beta}}{\psi(\alpha+1) - \psi(1)} + 1 \right) - \psi'\left(\alpha + \frac{H_0(t_i, \Theta) e^{\mathbf{X}_i^\top \beta}}{\psi(\alpha+1) - \psi(1)} + 1 \right) \omega_i}{\psi\left(\alpha + \frac{H_0(t_i, \Theta) e^{\mathbf{X}_i^\top \beta}}{\psi(\alpha+1) - \psi(1)} + 1 \right) - \psi\left(\frac{H_0(t_i, \Theta) e^{\mathbf{X}_i^\top \beta}}{\psi(\alpha+1) - \psi(1)} + 1 \right)} \\
&+ \sum_{i=1}^{n} \delta_i X_{ij} \tau_{i2} \left(\frac{\tau_{i1}}{\psi'(\alpha+1)} (\omega_i^2 - \omega_i') + \omega_i \right) \quad j = 1, 2, \ldots p. \qquad \text{(B.5)}
\end{aligned}
$$

B.5.4. Elements $j_{\beta_j\theta_k}$

$$
j_{\beta_j\theta_k} = \sum_{i=1}^{n} X_{ij} e^{\mathbf{X}_i^\top \beta} \frac{\frac{\partial}{\partial \theta_k} H_0(t_i, \Theta)}{\psi(\alpha+1) - \psi(1)} \left(\psi\left(\alpha + \frac{H_0(t_i, \Theta) e^{\mathbf{X}_i^\top \beta}}{\psi(\alpha+1) - \psi(1)} + 1 \right) - \psi\left(\frac{H_0(t_i, \Theta) e^{\mathbf{X}_i^\top \beta}}{\psi(\alpha+1) - \psi(1)} + 1 \right) \right)
$$

$$+ \sum_{i=1}^{n} X_{ij}\left(e^{\mathbf{X}_i^\top\beta}\right)^2 \frac{H_0(t_i,\Theta)\frac{\partial}{\partial\theta_k}H_0(t_i,\Theta)}{(\psi(\alpha+1)-\psi(1))^2}\left(\psi'\left(\alpha+\frac{H_0(t_i,\Theta)e^{\mathbf{X}_i^\top\beta}}{\psi(\alpha+1)-\psi(1)}+1\right)-\psi'\left(\frac{H_0(t_i,\Theta)e^{\mathbf{X}_i^\top\beta}}{\psi(\alpha+1)-\psi(1)}+1\right)\right)$$

$$- \sum_{i=1}^{n}\delta_i X_{ij}e^{\mathbf{X}_i^\top\beta}\frac{\frac{\partial}{\partial\theta_k}H_0(t_i,\Theta)}{\psi(\alpha+1)-\psi(1)}\left(\omega_i+\frac{\tau_{i1}}{\psi'(\alpha+1)}(\omega_i'-\omega_i^2)\right),\ j=1,2,\ldots,p,\ k=1,2,\ldots r. \quad \text{(B.6)}$$

B.5.5. Elements $j_{\theta_k\theta_{k'}}$

$$\begin{aligned} j_{\theta_k\theta_{k'}} =& -\sum_{i=1}^{n}\delta_i\frac{\frac{\partial^2}{\partial\theta_k\partial\theta_{k'}}h_0(t_i,\Theta)-\frac{\partial}{\partial\theta_k}h_0(t_i,\Theta)\frac{\partial}{\partial\theta_{k'}}h_0(t_i,\Theta)}{h_0^2(t_i,\Theta)}-\sum_{i=1}^{n}\delta_i e^{\mathbf{X}_i^\top\beta}\frac{\frac{\partial^2}{\partial\theta_k\partial\theta_{k'}}H_0(t_i,\Theta)}{\psi(\alpha+1)-\psi(1)}\omega_i \\ &+\sum_{i=1}^{n}\delta_i\left(e^{\mathbf{X}_i^\top\beta}\right)^2\frac{\frac{\partial}{\partial\theta_k}H_0(t_i,\Theta)\frac{\partial}{\partial\theta_{k'}}H_0(t_i,\Theta)}{(\psi(\alpha+1)-\psi(1))^2}(\omega_i^2-\omega_i') \\ &+\sum_{i=1}^{n}e^{\mathbf{X}_i^\top\beta}\frac{\frac{\partial^2}{\partial\theta_k\partial\theta_{k'}}H_0(t_i,\Theta)}{\psi(\alpha+1)-\psi(1)}\left(\psi\left(\alpha+\frac{H_0(t_i,\Theta)e^{\mathbf{X}_i^\top\beta}}{\psi(\alpha+1)-\psi(1)}+1\right)-\psi\left(\frac{H_0(t_i,\Theta)e^{\mathbf{X}_i^\top\beta}}{\psi(\alpha+1)-\psi(1)}+1\right)\right) \\ &+\sum_{i=1}^{n}\left(e^{\mathbf{X}_i^\top\beta}\right)^2\frac{\frac{\partial}{\partial\theta_k}H_0(t_i,\Theta)\frac{\partial}{\partial\theta_{k'}}H_0(t_i,\Theta)}{(\psi(\alpha+1)-\psi(1))^2}\left(\psi'\left(\alpha+\frac{H_0(t_i,\Theta)e^{\mathbf{X}_i^\top\beta}}{\psi(\alpha+1)-\psi(1)}+1\right)-\psi'\left(\frac{H_0(t_i,\Theta)e^{\mathbf{X}_i^\top\beta}}{\psi(\alpha+1)-\psi(1)}+1\right)\right). \end{aligned} \quad \text{(B.7)}$$

B.5.6. Elements $j_{\beta_j\beta_{j'}}$

$$\begin{aligned} j_{\beta_j\beta_{j'}} &= \sum_{i=1}^{n}X_{ij}X_{ij'}\frac{\tau_{i1}}{\psi'(\alpha+1)}\left(\psi\left(\alpha+\frac{H_0(t_i,\Theta)e^{\mathbf{X}_i^\top\beta}}{\psi(\alpha+1)-\psi(1)}+1\right)-\psi\left(\frac{H_0(t_i,\Theta)e^{\mathbf{X}_i^\top\beta}}{\psi(\alpha+1)-\psi(1)}+1\right)\right) \\ &+ \sum_{i=1}^{n}X_{ij}X_{ij'}\left(\frac{\tau_{i1}}{\psi'(\alpha+1)}\right)^2\left(\psi'\left(\alpha+\frac{H_0(t_i,\Theta)e^{\mathbf{X}_i^\top\beta}}{\psi(\alpha+1)-\psi(1)}+1\right)-\psi'\left(\frac{H_0(t_i,\Theta)e^{\mathbf{X}_i^\top\beta}}{\psi(\alpha+1)-\psi(1)}+1\right)\right) \\ &- \sum_{i=1}^{n}\delta_i X_{ij}X_{ij'}\frac{\tau_{i1}}{\psi'(\alpha+1)}\left(\omega_i+\frac{\tau_{i1}}{\psi'(\alpha+1)}(\omega_i'-\omega_i^2)\right),\quad j,j'=1,2,\ldots p. \end{aligned} \quad \text{(B.8)}$$

C. Asymptotic inference

The following analytical asymptotic results refer to the proportional hazards formulation described in Appendix B. Let $I_F(\boldsymbol{\Omega}) = \mathbb{E}\{J(\boldsymbol{\Omega})\}$ denote the corresponding Fisher information matrix. Under the usual regularity conditions for maximum likelihood estimation,

$$I_F(\boldsymbol{\Omega})^{1/2}\left(\widehat{\boldsymbol{\Omega}}-\boldsymbol{\Omega}\right)\xrightarrow{d}N(0,I),\qquad n\to\infty. \quad \text{(C.1)}$$

Consequently,

$$\widehat{\boldsymbol{\Omega}}\overset{a}{\sim}N\left(\boldsymbol{\Omega},\Sigma_{\boldsymbol{\Omega}}\right),\qquad \Sigma_{\boldsymbol{\Omega}}=I_F(\boldsymbol{\Omega})^{-1}.$$

In practice, standard errors under the proportional hazards model are obtained from the inverse observed information matrix evaluated at the maximum likelihood estimator. For the log-normal AFT

frailty specification, the marginal likelihood is evaluated numerically and standard errors are obtained from the inverse numerical Hessian of the integrated log-likelihood, as described in Section 3. For a generic scalar parameter ϑ_r, an approximate $(1-\rho)100\%$ confidence interval is

$$\widehat{\vartheta}_r \pm z_{1-\rho/2}\sqrt{\widehat{\mathrm{Var}}(\widehat{\vartheta}_r)}. \tag{C.2}$$

D. Particular forms of the EE frailty model

D.1. Weibull EE frailty model

Consider a Weibull regression model with scale parameter $\sigma > 0$ and regression parameter vector $\boldsymbol{\kappa} = (\kappa_1, \ldots, \kappa_p)^\top$. The baseline survival function conditional on the covariates is

$$S(t \mid \mathbf{X}) = \exp\left\{-\left(\frac{t}{\exp(\mathbf{X}^\top\boldsymbol{\kappa})}\right)^{1/\sigma}\right\}. \tag{D.1}$$

Defining $\theta = \frac{1}{\sigma}$ and $\boldsymbol{\beta} = -\frac{\boldsymbol{\kappa}}{\sigma}$, the corresponding hazard, cumulative hazard, and density functions can be written as $h(t \mid \mathbf{X}) = \theta t^{\theta-1}\exp(\mathbf{X}^\top\boldsymbol{\beta})$, $H(t \mid \mathbf{X}) = t^\theta \exp(\mathbf{X}^\top\boldsymbol{\beta})$, and

$$f(t \mid \mathbf{X}) = \theta t^{\theta-1}\exp(\mathbf{X}^\top\boldsymbol{\beta})\exp\left\{-t^\theta\exp(\mathbf{X}\top\boldsymbol{\beta})\right\}. \tag{D.2}$$

Substituting these expressions into the general EE frailty model yields the marginal survival function

$$S_m(t \mid \mathbf{X}) = \alpha B\left(\alpha, \frac{t^\theta\exp(\mathbf{X}^\top\boldsymbol{\beta})}{\psi(\alpha+1)-\psi(1)} + 1\right), \tag{D.3}$$

the marginal density function

$$\begin{aligned} f_m(t \mid \mathbf{X}) \;=\; & \frac{\alpha\theta t^{\theta-1}\exp(\mathbf{X}^\top\boldsymbol{\beta})}{\psi(\alpha+1)-\psi(1)} B\left(\alpha, \frac{t^\theta\exp(\mathbf{X}^\top\boldsymbol{\beta})}{\psi(\alpha+1)-\psi(1)} + 1\right)\left[\psi\left(\alpha + \frac{t^\theta\exp(\mathbf{X}^\top\boldsymbol{\beta})}{\psi(\alpha+1)-\psi(1)} + 1\right)\right. \\ & \left. -\psi\left(\frac{t^\theta\exp(\mathbf{X}^\top\boldsymbol{\beta})}{\psi(\alpha+1)-\psi(1)} + 1\right)\right], \end{aligned} \tag{D.4}$$

and the marginal hazard function

$$h_m(t \mid \mathbf{X}) = \frac{\theta t^{\theta-1}\exp(\mathbf{X}^\top\boldsymbol{\beta})}{\psi(\alpha+1)-\psi(1)}\left[\psi\left(\alpha + \frac{t^\theta\exp(\mathbf{X}^\top\boldsymbol{\beta})}{\psi(\alpha+1)-\psi(1)} + 1\right) - \psi\left(\frac{t^\theta\exp(\mathbf{X}^\top\boldsymbol{\beta})}{\psi(\alpha+1)-\psi(1)} + 1\right)\right]. \tag{D.5}$$

Finally, the corresponding log-likelihood function is obtained directly from (3.2) by replacing

$$h(t_i, \Theta, \boldsymbol{\beta}) = \theta t_i^{\theta-1}\exp(\mathbf{X}_i^\top\boldsymbol{\beta}),\; H(t_i, \Theta, \boldsymbol{\beta}) = t_i^\theta\exp(\mathbf{X}_i^\top\boldsymbol{\beta}). \tag{D.6}$$

D.2. Log-normal AFT EE frailty model

The log-normal specification used in the simulation study and empirical application is formulated as an accelerated failure time model. Given the frailty $V_i = v$ and covariates $\mathbf{X}_i$,

$$\log(T_i \mid V_i = v, \mathbf{X}_i) = \mu + \mathbf{X}_i^\top\boldsymbol{\beta} - \log(v) + \sigma Z_i, \qquad Z_i \sim N(0,1), \tag{D.7}$$

where $\sigma > 0$. Define

$$z_i(v) = \frac{\log(t_i) - \mu - \mathbf{X}_i^\top \boldsymbol{\beta} + \log(v)}{\sigma}. \tag{D.8}$$

The conditional density and survival functions are then

$$f(t_i \mid v, \mathbf{X}_i) = \frac{\phi\{z_i(v)\}}{\sigma t_i}, \qquad S(t_i \mid v, \mathbf{X}_i) = 1 - \Phi\{z_i(v)\}. \tag{D.9}$$

For an EE frailty with density $g_{EE}(v; \alpha)$, the corresponding marginal density is

$$f_m(t_i \mid \mathbf{X}_i) = \int_0^\infty \frac{\phi\{z_i(v)\}}{\sigma t_i} g_{EE}(v; \alpha)\, dv, \tag{D.10}$$

whereas the marginal survival function is

$$S_m(t_i \mid \mathbf{X}_i) = \int_0^\infty [1 - \Phi\{z_i(v)\}]\, g_{EE}(v; \alpha)\, dv. \tag{D.11}$$

Consequently, for right-censored survival data, the log-likelihood is

$$\ell_{\mathrm{AFT}} = \sum_{i=1}^{n} \log \left[\int_0^\infty \left\{ \frac{\phi\{z_i(v)\}}{\sigma t_i} \right\}^{\delta_i} \{1 - \Phi\{z_i(v)\}\}^{1-\delta_i}\, g_{EE}(v; \alpha)\, dv \right]. \tag{D.12}$$

Because the frailty appears inside $z_i(v)$ through $\log(v)$, these integrals do not reduce to the Laplace-transform expressions available under the multiplicative-hazard formulation. They are therefore evaluated numerically using Gauss-Laguerre quadrature. The score vector and observed Hessian for this AFT specification are likewise evaluated numerically and are not represented by the analytical expressions in Appendix B.



AIMS Press

© 2026 the Author(s), licensee AIMS Press. This is an open access article distributed under the terms of the Creative Commons Attribution License (http://creativecommons.org/licenses/by/4.0)